

## Changes in vegetation net primary productivity from 1982 to 1999 in China

Shilong Piao,<sup>1,2</sup> Jingyun Fang,<sup>1,2</sup> Liming Zhou,<sup>3</sup> Biao Zhu,<sup>1</sup> Kun Tan,<sup>1</sup> and Shu Tao<sup>4</sup>

Received 31 March 2004; revised 3 March 2005; accepted 4 May 2005; published 22 June 2005.

[1] Terrestrial net primary production (NPP) has been a central focus of ecosystem science in the past several decades because of its importance to the terrestrial carbon cycle and ecosystem processes. Modeling studies suggest that terrestrial NPP has increased in the northern middle and high latitudes in the past 2 decades, and that such increase has exhibited seasonal and spatial variability, but there are few detailed studies on the temporal and spatial patterns of NPP trend over time in China. Here we present the trends in China's terrestrial NPP from 1982 to 1999 and their driving forces using satellite-derived NDVI (Normalized Difference Vegetation Index), climate data, and a satellite-based carbon model, CASA (Carnegie-Ames-Stanford Approach). The majority of China (86% of the study area) has experienced an increase in NPP during the period 1982–1999, with an annual mean increase rate of 1.03%. This increase was resulted primarily from plant growth in the middle of the growing season (June to August) (about 43.2%), followed by spring (33.7%). At the national and biome levels, the relative increase is largest in spring (March–May), indicating an earlier onset of the growing season. The changes in the phase of China's seasonal NPP curve may primarily be the result of advanced growing season (earlier spring) and enhanced plant growth in summer. During the past 2 decades the amplitude of the seasonal curve of NPP has increased and the annual peak NPP has advanced. Historical NPP trends also indicated a high degree of spatial heterogeneity, coupled with regional climate variations, agricultural practices, urbanization, and fire disturbance.

**Citation:** Piao, S., J. Fang, L. Zhou, B. Zhu, K. Tan, and S. Tao (2005), Changes in vegetation net primary productivity from 1982 to 1999 in China, *Global Biogeochem. Cycles*, 19, GB2027, doi:10.1029/2004GB002274.

### 1. Introduction

[2] The drafting of the Kyoto Protocol ignited an unprecedented effort in biogeochemical sciences [Schulze *et al.*, 2000]. As a key component of the terrestrial carbon cycle and ecosystem process, terrestrial net primary production (NPP) uniquely integrates climatic, ecological, and human-induced influences on the global carbon cycle [Nemani *et al.*, 2003; Potter *et al.*, 2003]. Its alteration greatly affects CO<sub>2</sub> exchange between the land and the atmosphere and thus global climate [Keeling *et al.*, 1996; Cramer *et al.*, 1999]. Therefore variations in NPP and its interactions with

global climates have been one of the key focuses of ecological study in the past 3 decades [e.g., Melillo *et al.*, 1993; Field *et al.*, 1998; Cramer *et al.*, 2001; Hicke *et al.*, 2002a, 2002b; Liu *et al.*, 2002; Cao *et al.*, 2003; Fang *et al.*, 2003].

[3] Terrestrial ecosystem production cannot be directly measured at the regional or global scales, and thus its estimation by computer models has become indispensable [Cramer *et al.*, 1999]. During the past decades, several types of models have been developed to estimate NPP at large scales, such as TEM [Raich *et al.*, 1991; Melillo *et al.*, 1993], CASA [Potter *et al.*, 1993; Field *et al.*, 1995], Century [Parton *et al.*, 1993], BIOME3 [Haxeltine and Prentice, 1996], and BIOME-BGC [Running and Hunt, 1993]. Among these models, satellite-based NPP models provide an effective approach for exploring dynamic changes in NPP and their spatiotemporal variations at regional and global scales [Potter *et al.*, 1993; Ruimy *et al.*, 1994; Field *et al.*, 1995; Prince and Goward, 1995; Malmström *et al.*, 1997; Field *et al.*, 1998; Randerson *et al.*, 1999; Hicke *et al.*, 2002a, 2002b; Fang *et al.*, 2003; Nemani *et al.*, 2003], because satellite data provide information about the integrated responses of plant canopies to environ-

<sup>1</sup>Department of Ecology, College of Environmental Sciences, Center for Ecological Research and Education, Peking University, Beijing, China.

<sup>2</sup>Also at Key Laboratory for Earth Surface Processes of the Ministry of Education, Peking University, Beijing, China.

<sup>3</sup>School of Earth and Atmospheric Sciences, Georgia Institute of Technology, Atlanta, Georgia, USA.

<sup>4</sup>Key Laboratory for Earth Surface Processes of the Ministry of Education, Peking University, Beijing, China.

mental factors, including those that might otherwise be omitted from model algorithms, such as land use change, CO<sub>2</sub> and N fertilization, irrigation, and fire [Malmström *et al.*, 1997; Hicke *et al.*, 2002a]. Moreover, the development of a multiyear continuous data set of normalized difference vegetation index (NDVI) derived from the Advanced Very High Resolution Radiometer (AVHRR) on the National Oceanic and Atmospheric Administration (NOAA) satellite sensors has greatly improved the ability to estimate the year-to-year changes in regional and global scale terrestrial production [Malmström *et al.*, 1997; Behrenfeld *et al.*, 2001; Myneni *et al.*, 2001; Tucker *et al.*, 2001; Zhou *et al.*, 2001; Dong *et al.*, 2003; Piao *et al.*, 2003; Stow *et al.*, 2004].

[4] Some studies have modeled NPP responses to climate changes at large scales using AVHRR NDVI data sets and concluded that terrestrial photosynthetic activity in northern middle and high latitudes has increased over the past 2 decades [i.e., Behrenfeld *et al.*, 2001; Hicke *et al.*, 2002a; Lucht *et al.*, 2002; Fang *et al.*, 2003; Nemani *et al.*, 2003]. Mechanisms for such increase, however, remain largely uncertain, especially at regional scale [Schimel *et al.*, 2001] since the drivers of changes in NPP exhibit considerable spatial and temporal variability in responses to global climate change [Keeling *et al.*, 1996; Myneni *et al.*, 1997a; Zhou *et al.*, 2001; Dong *et al.*, 2003].

[5] Located in the eastern monsoon region of Eurasia, China encompasses a wide range of climates and a variety of topographies, which make it an ideal region in which to study responses of vegetation to climate changes. In eastern China, climate changes from tropical, through subtropical, warm temperate, and temperate, to cool temperate (subarctic) from south to north, and correspondingly, vegetation is rain/seasonal forests, evergreen broadleaf forests, deciduous broadleaf forests, and deciduous and evergreen needleleaf forests [Fang *et al.*, 2002]. In the northern inland areas, the climate is dry and forms a humid/arid climate sequence of humid, semihumid, semiarid, and arid from east to west, and therefore the vegetation type changes from forest, forest grasslands, grasslands to deserts [Fang *et al.*, 2002].

[6] China has experienced significant climate changes [Zhai *et al.*, 1999; Chinese Climate Change National Research Group, 2000] and extensive changes in land use and land cover due to its “reform and opening” policies, especially in the eastern coastal regions, during the past 2 decades [Liu *et al.*, 2003]. These changes may have resulted in large variations in China’s terrestrial ecosystem production. Therefore investigating variations in NPP of China will advance our understanding of how human-induced and natural changes interact with ecosystem processes. Although there have already been several such studies [e.g., Ni, 2000; Cao *et al.*, 2003; Fang *et al.*, 2003], most of them have used climate-based approaches but few have examined seasonal patterns of NPP trends over time despite their importance to understand the mechanisms for NPP variation and carbon cycles. To investigate where, when, and why NPP changed in China, here we used an NDVI-based carbon model, CASA (Carnegie-Ames-Stanford Approach) [Potter *et al.*, 1993; Field *et al.*, 1995], and a number of surface observations to explore interannual variations of

annual, seasonal, and monthly terrestrial NPP and their possible drivers in China from 1982 to 1999.

## 2. Data and Methods

### 2.1. CASA Model

[7] Theoretically, vegetation NPP can be estimated using the variables of the photosynthetically active radiation absorbed by green vegetation (APAR) and the efficiency by which that radiation is converted to plant biomass increment ( $\epsilon$ ) [Monteith, 1977]. In the CASA, the incident photosynthetically active radiation (PAR) and the fraction of absorbed photosynthetically active radiation (FAPAR) determine APAR. Light-use efficiency ( $\epsilon$ ) is estimated as the maximum light-use efficiency variable ( $\epsilon^*$ ), and vegetation light-use efficiency stressed by temperature ( $T$ ) and moisture ( $W$ ). For a geographic coordinate ( $x$ ) at month  $t$ , NPP is estimated as

$$\text{NPP}(x, t) = \text{FAPAR}(x, t) \times \text{PAR}(x, t) \times \epsilon^*(x, t) \times T(x, t) \times W(x, t), \quad (1)$$

where solar radiation is converted to PAR by multiplying by 0.5. The FAPAR is calculated as a linear function of the NDVI simple ratio ( $SR$ ),

$$\text{SR}(x, t) = [1 + \text{NDVI}(x, t)] / [1 - \text{NDVI}(x, t)] \quad (2)$$

$$\text{FAPAR}(x, t) = \min \left[ \frac{\text{SR}(x, t) - \text{SR}_{\min}}{\text{SR}_{\max} - \text{SR}_{\min}}, 0.95 \right], \quad (3)$$

where  $\text{SR}_{\min}$  represents  $SR$  for unvegetated land areas and is set to 1.08 for all grid cells [Potter *et al.*, 1993]. In dependent of vegetation,  $\text{SR}_{\max}$  is set between 4.14 and 6.17.

[8] The  $\epsilon^*$  was set to 0.405 following the calibration and validation procedures described by Potter *et al.* [1993]. The values of  $\epsilon^*$  will alter NPP and magnitude of its trends, but the relative trend will not change. The temperature stress impact factor is computed using monthly mean temperature and optimal temperatures ( $T_{\text{opt}}$ ) for plant production, the temperature during the month of maximum NDVI [Potter *et al.*, 1993]. The model uses monthly averaged climate data and soil texture information to calculate the influence of moisture stress on light-use efficiency through a one-layer bucket soil moisture model. Details about this model are described by Potter *et al.* [1993] and Field *et al.* [1995].

[9] Fang *et al.* [2003] have validated CASA-derived NPP in China by comparing the annual NPP trends for cultivated crops and forests with those estimated from China’s food-yield statistics and forest inventory surveys, and found that the two results were highly consistent. Terrestrial NPP fluxes from the CASA model also validated against seasonal patterns of atmospheric CO<sub>2</sub> measurements at flask sampling stations around the world [Denning, 1994; Potter *et al.*, 1999].

### 2.2. NDVI Data Set

[10] NDVI uses red and near-infrared surface reflectance of the canopy to signal the abundance and energy absorp-

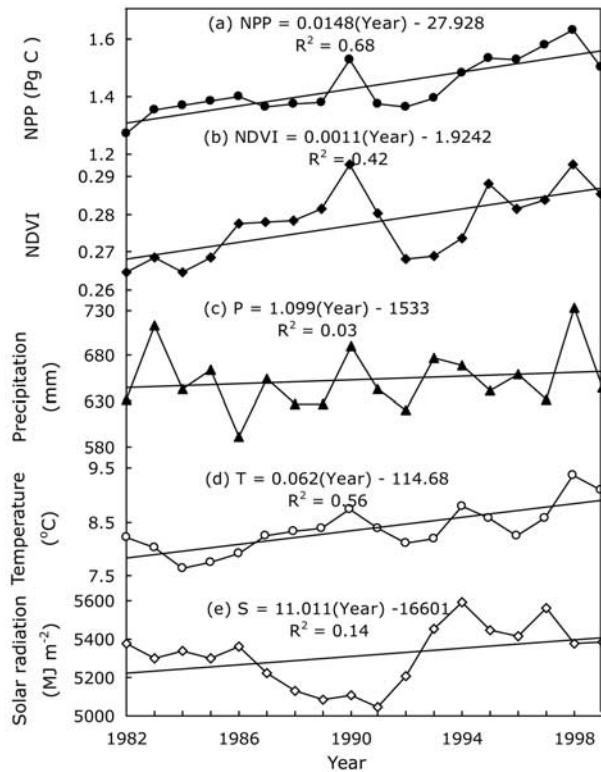


**Figure 1.** Interannual changes in: (a) total terrestrial net primary production (NPP,  $\text{PgC yr}^{-1}$ ) in China estimated from CASA; (b) area-weighted mean normalized difference vegetation index (NDVI); (c) annual precipitation (mm), (d) annual mean temperature ( $^{\circ}\text{C}$ ), and (e) annual solar radiation.

tion by leaf pigments such as chlorophyll. It is expressed on a scale between  $-1$  and  $+1$ . The NDVI data set used in this study was for the period 1982–1999 and was the standard 8-km bimonthly continental product of Global Inventory Monitoring and Modeling Studies (GIMMS) group [Tucker *et al.*, 2001; Zhou *et al.*, 2001; Slayback *et al.*, 2003]. The processing of this data set includes improved navigation, calibration for sensor degradation, and correction for stratospheric volcanic aerosols from El Chichon and Mount Pinatubo eruptions in April 1984 and June 1991 [Zhou *et al.*, 2001; Slayback *et al.*, 2003]. Further details on the quality of the GIMMS NDVI data set can be found in the work of Los [1988] and Tucker *et al.* [2001]. Although some researchers questioned the quality of the AVHRR NDVI time series [e.g., Gutman, 1999], a number of studies have suggested that the data set is suitable for identifying long-term trends in vegetation activity [e.g., Tucker *et al.*, 2001; Zhou *et al.*, 2001, 2003; Piao *et al.*, 2003; Slayback *et al.*, 2003].

[11] Monthly NDVI was obtained by choosing the monthly maximum value which can further eliminate the disturbance from cloud, atmosphere, and changes in solar altitude angle [Holben, 1986; Tucker *et al.*, 1994]. Furthermore, in order to minimize the impact of soil variations in bare and sparsely vegetated regions, only regions with an annual mean NDVI of  $>0.1$  during the 18 years were

used in this study. For this reason, the total study area in this study was  $803 \times 10^4 \text{ km}^2$ , 85.5% of China's land area ( $940 \times 10^4 \text{ km}^2$ ).

### 2.3. Climate Data Sets

[12] The meteorological data required as input for the CASA included monthly mean temperature, precipitation, and solar radiation data. These data sets, with a spatial resolution of  $0.1^{\circ}$  for 1982–1999, were obtained from Fang *et al.* [2001a, 2003] and Piao *et al.* [2003]. The temperature and precipitation data sets were produced from 680 well-distributed climate stations across China [Piao *et al.*, 2003]. Solar radiation data set was generated from 98 solar radiation observation stations over all the country [Fang *et al.*, 2001a, 2003]. These climate and solar radiation stations were evenly distributed over most regions of the study area, but not the Tibetan Plateau. Therefore some errors might result from the interpolation in the plateau due to limited stations available [Piao *et al.*, 2003].

### 2.4. Information on Vegetation and Soil

[13] Soil texture and vegetation type were required as the inputs of the CASA. In this study, the former was obtained by digitizing the soil texture map of China [Institute of Soil Science, 1986], and the latter was based on the vegetation map of China [Institute of Geography, 1996]. As required by the CASA, 11 types were obtained from the vegetation map, namely, evergreen broadleaf forests, deciduous broadleaf forests, broadleaf and needleleaf mixed forests, evergreen needleleaf forests, deciduous needleleaf forests, broadleaf shrubs, temperate grasslands, savannas, alpine meadows and tundra, deserts, and cultivation.

## 3. Results

### 3.1. Annual NPP Trends

#### 3.1.1. Trends at the Country Scale

[14] Figure 1 shows interannual changes in (Figure 1a) total terrestrial NPP, (Figure 1b) area-weighted NDVI, (Figure 1c) annual mean precipitation, (Figure 1d) annual mean temperature, and (Figure 1e) solar radiation in China. On average, China's NPP increased significantly from 1982 to 1999 ( $R^2 = 0.68$ ,  $p < 0.001$ ), with a total increase rate of 18.5% or an annual mean increase rate of 1.03%.

[15] Interannual variations in NPP corresponded closely with NDVI ( $R^2 = 0.62$ ,  $p < 0.001$ ) and temperature ( $R^2 = 0.52$ ,  $p = 0.001$ ) (Figures 1b and 1d). Over the 18 years, annual mean NDVI and temperature rose substantially, with rates of 0.0011 ( $R^2 = 0.42$ ,  $p = 0.004$ ) and  $0.062^{\circ}\text{C}$  per year ( $R^2 = 0.56$ ,  $p < 0.001$ ), respectively. No apparent trend was found for precipitation ( $R^2 = 0.03$ ,  $p = 0.492$ ) and solar radiation ( $R^2 = 0.14$ ,  $p = 0.134$ ). NPP and NDVI were anomalously high in 1990 and 1998, strongly linked with warm temperatures and high precipitation. As a result of volcanic eruptions of Mount Pinatubo in 1991, stratospheric aerosols greatly increased and thus caused a considerable decline of temperature and solar radiation in 1992 [Stowe *et al.*, 1992; Minnis *et al.*, 1993]. In addition, low precipitation in 1992 led possibly to low NDVI and NPP in this year.

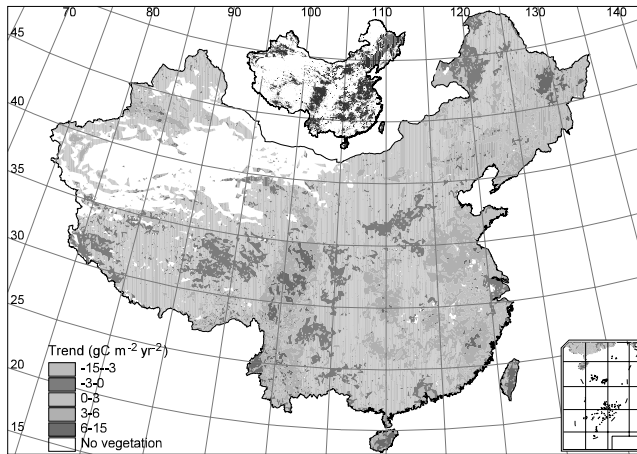


**Figure 2.** Spatial distribution of annual NPP trend calculated from CASA over 1982 to 1999. The insert map at top shows significant increase (blue) or decrease (red) in NDVI over the 18 years. See color version of this figure at back of this issue.

These results indicate that temperature and precipitation are likely major drivers of dynamic changes in terrestrial NPP at the country scale.

### 3.1.2. Spatial Patterns of Trends

[16] We estimated linear trends of NPP for each pixel using ordinary least squares to demonstrate spatiotemporal changes in NPP. Figure 2 shows spatial patterns of the estimated NPP trend from 1982 to 1999. Despite its large increase as a whole, China's NPP shows a remarkable geographical heterogeneity in NPP trends. Overall, NPP increased over 86% and significantly over 33% ( $p < 0.05$ ) of the study area, and decreased significantly over only 0.6% ( $p < 0.05$ ) of the study area.

[17] The significant increase in NPP mainly occurred in mountainous and agricultural regions of China. These regions are: (1) eastern humid areas under the influence of southeast monsoon, including Hainan Island, Taiwan, and Wuyishan Mountain, with an annual mean increase of over  $6 \text{ g C m}^{-2} \text{ yr}^{-2}$ ; (2) northwestern Sichuan Province and southwestern Yunnan Province under the influence of southwest monsoon, with an annual mean increase of over  $6 \text{ g C m}^{-2} \text{ yr}^{-2}$ ; and (3) main agricultural areas in eastern China, including parts of the Northeast China Plain, the North China Plain, and the Yangtze River Basin, with an annual mean increase of  $3\text{--}6 \text{ g C m}^{-2} \text{ yr}^{-2}$ . A marked increase in annual NPP was also seen over Northeast China Plain, Xiao-xing-an-ling Mountains in the northeast region, and Tianshan-Artai Mountains in the northwest region.

[18] On the other hand, western Tibet, the source of the Yangtze River, the boundary area of Guizhou and Guangxi Provinces, and grasslands in northeast China all experienced an insignificant decrease in annual NPP. The Pearl River and Yangtze River deltas are among the few regions with significant decreases in annual NPP, and such decrease is largest in the Pearl River delta with an annual mean magnitude larger than  $3 \text{ g C m}^{-2} \text{ yr}^{-2}$ .

### 3.1.3. Trends by Vegetation Type

[19] We investigate interannual NPP changes for all 11 vegetation types described in section 2. The NPP for all vegetation types except deciduous needleleaf forests shows an increase over the past 18 years ( $R^2 = 0.26$  to  $0.67$ ,  $p < 0.03$ ) (Table 1). No significant trend ( $R^2 = 0.03$ ,  $p = 0.502$ ) is observed for deciduous needleleaf forests in the northernmost of northeast China, probably due to a heavy forest fire in 1987 and continuous logging [Zhou, 1997]. The NPP increase rates by vegetation type were qualitatively similar to those at the country scale (Table 1). The largest increase in NPP occurred in broadleaf and needleleaf mixed forests with an annual mean magnitude of  $4.23 \text{ g C m}^{-2} \text{ yr}^{-2}$ , while the smallest was located in desert ( $0.59 \text{ g C m}^{-2} \text{ yr}^{-2}$ ) (Table 1). The mean increase rate of NPP for most vegetation types was close to 1% per year, which supports the annual mean increasing rate of 1% over the whole country (Figure 1). Relative change values suggest that the largest NPP variation ( $\text{CV} = 11.1\%$ ) occurs in deserts (Table 1).

[20] Furthermore, annual NPP trends for each vegetation type were divided into four types: insignificant increase, insignificant decrease, significant increase, and significant decrease. For each vegetation type, the ratios of areas for each type to the total are shown in Figure 3. More than 75% of the total area for all 11 vegetation types experienced significant increases in annual NPP. Only a small percentage of the area showed a significant decrease for these vegetation types, with the largest decrease in cultivation (1.4%) and the smallest increase in deciduous needleleaf forests (8.9%). Broadleaf and needleleaf mixed forests and cultivation had the largest percentage of area with significant increase in annual NPP, at 63.6% and 45%, respectively.

## 3.2. Seasonal NPP Trends

### 3.2.1. Seasonal Trends at the Country Scale

[21] The total NPP of China's vegetation showed a remarkable seasonal variation. The 18-year average NPP values are largest in summer (June to August), about  $0.87 \text{ Pg C}$  (about 61% of the total annual NPP), followed by autumn (September to November,  $0.29 \text{ Pg C}$ ), spring (March to May,  $0.23 \text{ Pg C}$ ), and winter (December to February,  $0.04 \text{ Pg C}$ ). Figure 4 illustrates the changes in total NPP, mean NDVI, mean temperature, mean precipitation, and solar radiation in the four seasons during the study period. Evidently, the total NPP increased during all seasons, especially in spring, summer, and autumn ( $p < 0.05$ ).

[22] Spring shows the most significant increase in NPP of any season ( $R^2 = 0.49$ ,  $p = 0.001$ ). The total NPP increased from  $0.20 \text{ Pg C}$  in the early 1980s (average of 1982–1984) to  $0.30 \text{ Pg C}$  in the late 1990s (average of 1997–1999) with a trend of 2.16% or  $5.0 \text{ Tg C per year}$  (33.7% of the total annual increase in NPP). Such an increase may be associated with temperature rise in spring, resulting in advanced growing season [Zhou et al., 2001; Piao et al., 2003]. Spring NPP was significantly correlated with spring temperature ( $R^2 = 0.78$ ,  $p < 0.001$ ) but not with spring precipitation ( $R^2 = 0.11$ ,  $p = 0.170$ ) and spring solar radiation ( $R^2 = 0.08$ ,  $p = 0.258$ ). Both mean temperature and NDVI increased pronouncedly by  $0.06^\circ\text{C yr}^{-1}$  ( $R^2 =$

**Table 1.** Annual NPP Total and Its 18-Year Average for 11 Vegetation Types in China From 1982 to 1999, Together With Their Total Area, Annual Mean NPP, and Trend and Trend Rate of Annual Mean NPP<sup>a</sup>

	EBF	DBF	BNMF	ENF	DNF	Shrubs	Grasslands	Savannas	AMT	Deserts	Cultivation	Total
1982	105.8	53.8	10.1	125.2	38.6	42.5	132.6	302.3	205.4	24.4	232.4	1273.0
1983	114.7	50.7	8.2	139.3	28.8	49.0	137.1	330.4	208.7	25.6	259.7	1352.2
1984	111.1	50.9	8.8	137.3	31.2	49.6	151.1	320.8	212.2	26.4	267.2	1366.6
1985	118.7	51.7	8.2	140.3	34.6	51.5	142.6	332.6	215.8	25.9	262.9	1384.8
1986	123.2	51.6	8.6	144.6	33.6	49.4	139.2	333.6	211.9	27.4	275.0	1397.9
1987	111.6	54.7	9.2	129.7	32.9	46.4	147.1	330.0	190.1	28.9	281.3	1361.9
1988	103.8	52.9	9.1	128.6	36.6	45.9	162.6	306.5	226.3	33.8	267.9	1374.1
1989	115.4	58.5	10.3	134.4	40.4	47.1	145.2	331.1	199.6	26.6	268.9	1377.5
1990	126.4	60.6	10.7	153.7	31.4	50.8	168.0	362.9	216.3	29.5	316.6	1526.8
1991	105.7	60.7	11.0	128.8	36.4	43.5	154.1	324.0	196.1	28.7	285.9	1374.9
1992	107.2	53.8	10.5	128.5	32.6	44.9	145.4	322.1	195.5	28.1	292.9	1361.5
1993	105.9	56.3	9.7	127.9	30.7	45.5	164.3	324.5	213.2	30.7	287.3	1396.0
1994	113.1	53.9	9.8	145.0	32.9	51.9	167.8	334.7	248.6	33.4	291.3	1482.4
1995	127.2	60.8	11.4	159.1	36.5	53.9	150.9	370.2	221.4	28.0	310.8	1530.3
1996	131.4	59.4	11.4	158.7	36.9	50.9	164.2	366.5	226.4	31.1	291.2	1528.0
1997	133.6	62.5	10.0	163.0	47.6	55.4	160.6	380.2	223.2	32.2	308.5	1577.0
1998	130.0	61.0	11.8	160.6	28.6	57.7	175.1	391.8	245.5	35.8	330.1	1628.1
1999	119.4	57.6	10.1	149.0	34.3	52.5	159.5	349.5	243.2	33.0	294.3	1502.4
Mean, TgC yr <sup>-1</sup>	116.9	56.2	9.9	141.9	34.7	49.4	153.7	339.6	216.6	29.4	284.7	1433.1
CV, %	8.4	7.1	11.0	9.1	13.1	8.4	7.9	7.4	7.8	11.1	8.2	6.7
R	0.51	0.74	0.69	0.62	0.17	0.57	0.74	0.72	0.60	0.78	0.82	0.82
Total area, 10 <sup>6</sup> ha	27.97	22.93	3.36	57.84	12.19	19.15	106.28	151.52	154.47	80.40	166.73	802.84
Mean NPP, g C m <sup>-2</sup> yr <sup>-1</sup>	417.9	245.1	296.0	245.3	284.6	257.8	144.7	224.2	140.3	36.6	170.7	178.5
Trend, g C m <sup>-2</sup> yr <sup>-2</sup>	3.34	2.40	4.23	2.59	1.18	2.33	1.59	2.22	1.24	0.59	2.16	1.84
Mean increase Rate, % yr <sup>-1</sup>	0.80	0.98	1.43	1.06	0.42	0.90	1.10	0.99	0.88	1.61	1.27	1.03

<sup>a</sup>Note that NPP is calculated from a carbon model, CASA (Carnegie-Ames-Stanford Approach). EBF, evergreen broadleaf forests; DBF, deciduous broadleaf forests; BNMF, broadleaf and needleleaf mixed forests; ENF, evergreen needleleaf forests; DNF, deciduous needleleaf forests; AMT, alpine meadows and tundra.

0.47,  $p = 0.002$ ) and  $0.0018 \text{ yr}^{-1}$  ( $R^2 = 0.40$ ,  $p = 0.005$ ), respectively, and were larger than those in summer and autumn. No apparent trend was present for precipitation ( $R^2 = 0.0048$ ,  $p = 0.785$ ) and solar radiation ( $R^2 = 0.09$ ,  $p = 0.240$ ).

[23] Summer has the largest NPP increase in magnitude, with a trend of 6.4 Tg C per year or 43.2% of the total

annual NPP increase. The concurrent increase in summer rainfall and temperature may be the main driver for such increase. Both mean summer precipitation and temperature rose remarkably in spite of a large fluctuation ( $R^2 = 0.27$ ,  $p = 0.027$  and  $R^2 = 0.37$ ,  $p = 0.007$ , respectively). However, the increasing rate of summer NPP was the smallest (only 0.7% per year), mainly owing to the large initial NPP value.

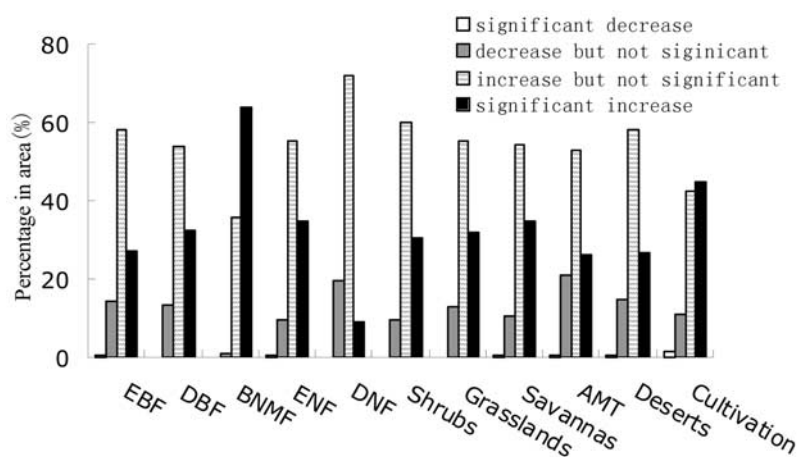


**Figure 3.** Area percentage of significant increase, significant decrease, insignificant increase, and insignificant decrease in annual NPP derived from CASA for all 11 vegetation types in China from 1982 to 1999. EBF, evergreen broadleaf forests; DBF, deciduous broadleaf forests; BNMF, broadleaf and needleleaf mixed forests; ENF, evergreen needleleaf forests; DNF, deciduous needleleaf forests; AMT, alpine meadows and tundra.

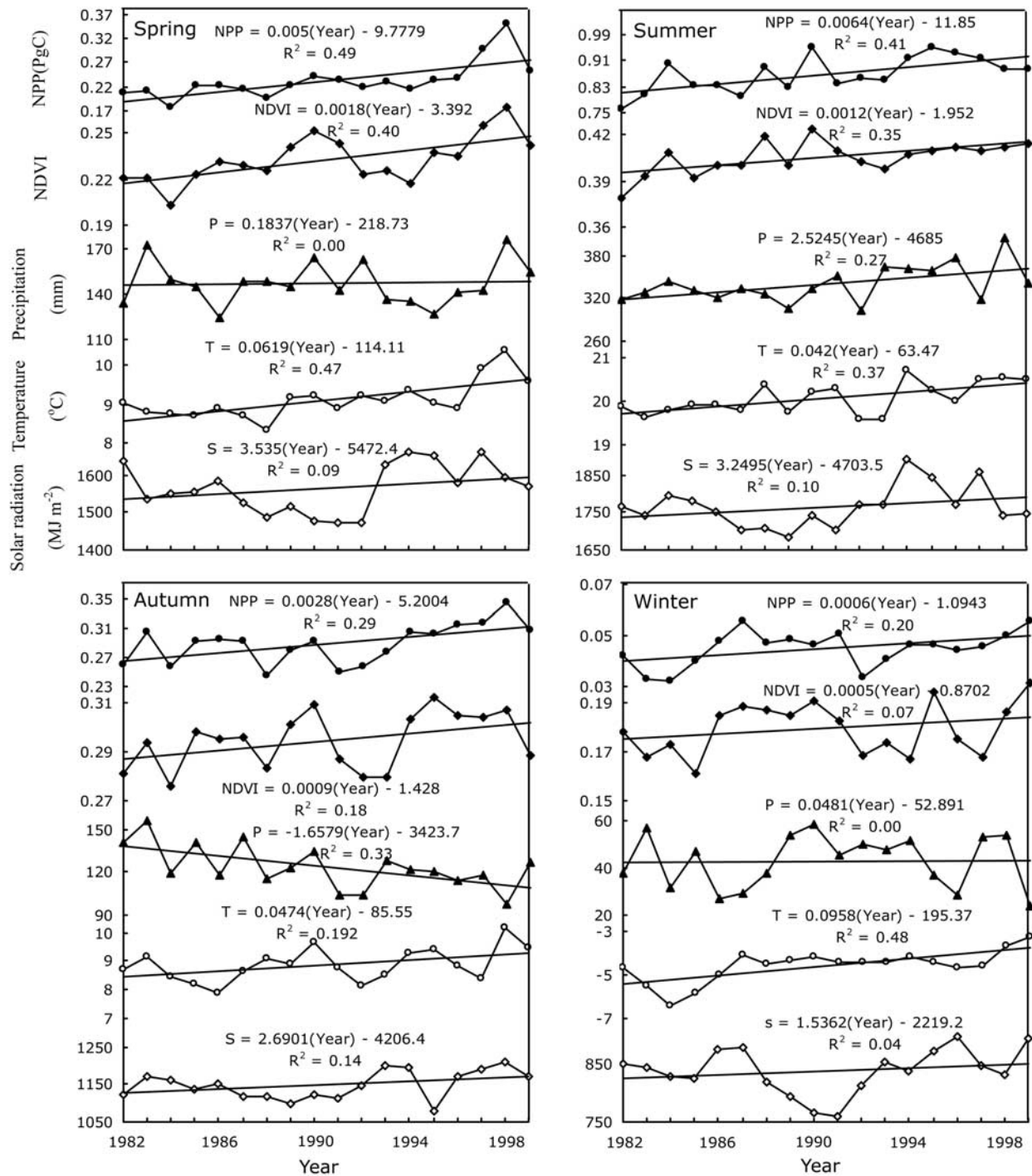


**Figure 4.** Interannual changes in CASA-derived total NPP, averaged NDVI, averaged precipitation, averaged temperature, and solar radiation in China for four seasons during 1982–1999.

Summer solar radiation did not show significant trend ( $R^2 = 0.10$ ,  $p = 0.206$ ).

[24] Annual mean increase in autumn NPP was about 2.8 Tg C, with a mean increase rate of  $1.0\% \text{ yr}^{-1}$ . Both autumn mean temperature and NDVI exhibited significant

increasing trends with smaller rates than those in spring. However, precipitation decreased significantly ( $R^2 = 0.33$ ,  $p = 0.012$ ). Autumn NPP was significantly correlated with summer precipitation of the same year ( $R^2 = 0.26$ ,  $p = 0.029$ ), but insignificantly with autumn temperature ( $R^2 =$

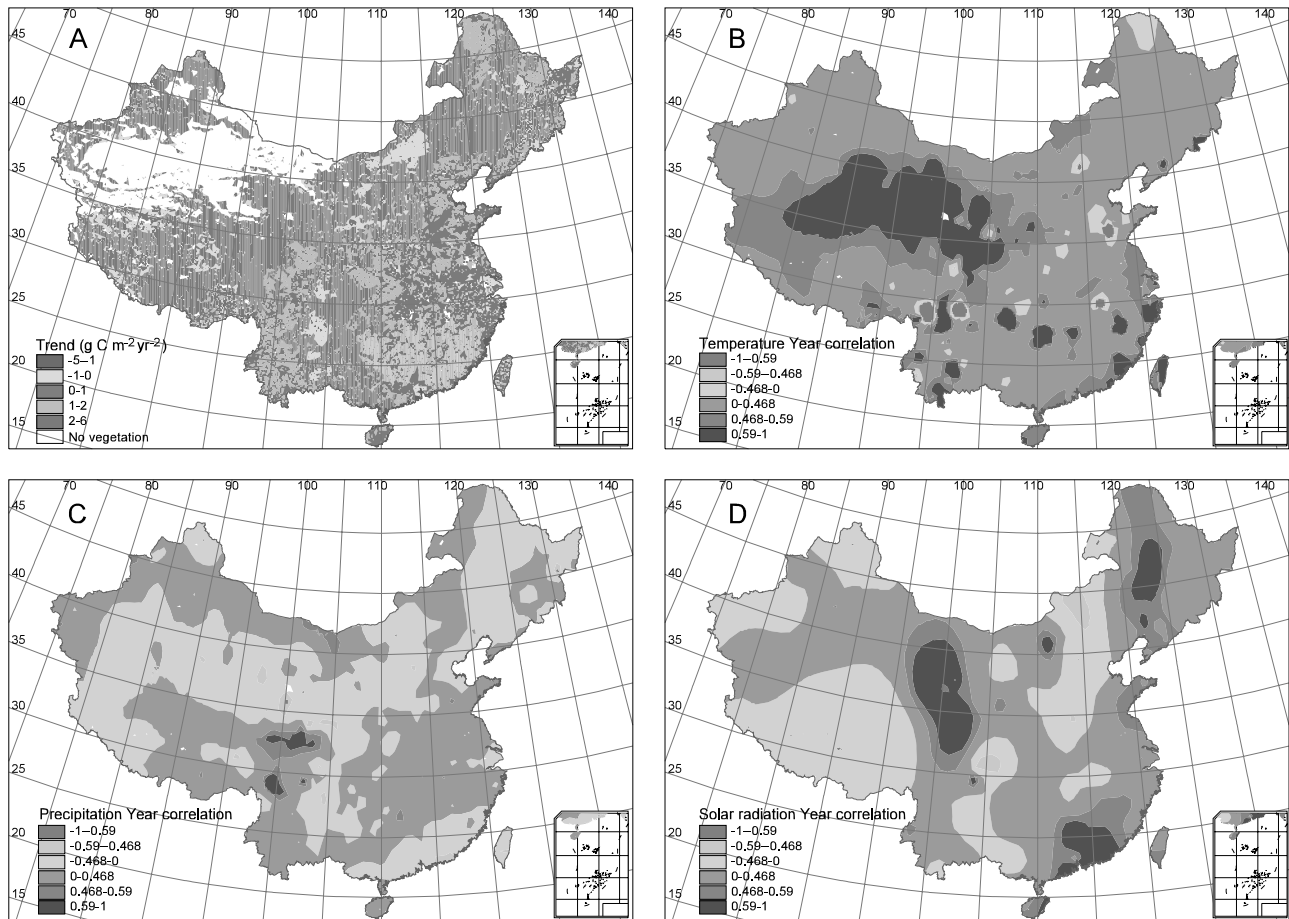


**Figure 5.** Spatial patterns of (a) trends in CASA-derived mean NPP, and coefficients of correlation (b) between temperature and time, (c) between precipitation and time, and (d) between solar radiation and time for each grid cell for spring (March to May) in China. The value of 0.468 and 0.59 for coefficient of correlation in the legend of Figures 5b, 5c, and 5d corresponds statistically to 5% and 1% significance levels, respectively. See color version of this figure at back of this issue.

0.21,  $p = 0.052$ ) and precipitation ( $R^2 = 0.00$ ,  $p = 0.097$ ), suggesting a lagged response of vegetation activity in autumn to precipitation in summer.

[25] Winter mean temperature increased significantly over the 18 years ( $R^2 = 0.48$ ,  $p = 0.002$ ), with the mean rate of  $0.1^\circ\text{C yr}^{-1}$  larger than that in other seasons. As expected, the mean magnitude of NPP increase was the smallest among all the four seasons, accounting for only 0.4% of the total annual mean increase of NPP ( $0.6 \text{ Tg C}$ ) probably because of the nongrowing status for most vegetation types in China during winter.

### 3.2.2. Spatial Patterns in Seasonal NPP Trends

[26] The NPP values for non-evergreen vegetation types are typically zero in winter and thus we only consider NPP during the growing season (spring, summer, and autumn) to explore geographical distributions of the interannual NPP variations in different seasons over the 18 years. NPP trends in spring (Figure 5a) show that more than 88% of the study area exhibited an increase in NPP (about 30% with a significant increase), owing possibly to the warming-promoted earlier spring over most of China. More than

97% of our study region experienced an increase in spring temperature (49.3% with a significant increase) (Figure 5b). Consequently, spring NPP increased with an annual trend of  $1.0 \text{ g C m}^{-2} \text{ yr}^{-2}$  in the eastern humid areas under the southeast monsoon, southwestern Sichuan and southwestern Yunnan under the southwest monsoon, the Northeast China Plain, and the North China Plain. The NPP increase in these areas was coupled with an increased spring temperature (Figure 5b) and solar radiation (Figure 5d). Only a few areas, including the center of the Inner Mongolia Plateau, the Pearl River, and Yangtze River deltas, exhibited a decrease in NPP. This decrease in the center of the Inner Mongolia Plateau may be related to the decreased precipitation in this area (Figure 5c).

[27] In summer, more areas have experienced NPP decrease and less areas showing significant increase, compared with in spring (Figure 6a). Over the 18 years, the area with insignificant increase, significant increase, and significant decrease in summer NPP accounted for 74%, 20%, and 1.0% of the study area, respectively. The summer NPP had increased in the plain areas, Xiao-xing-

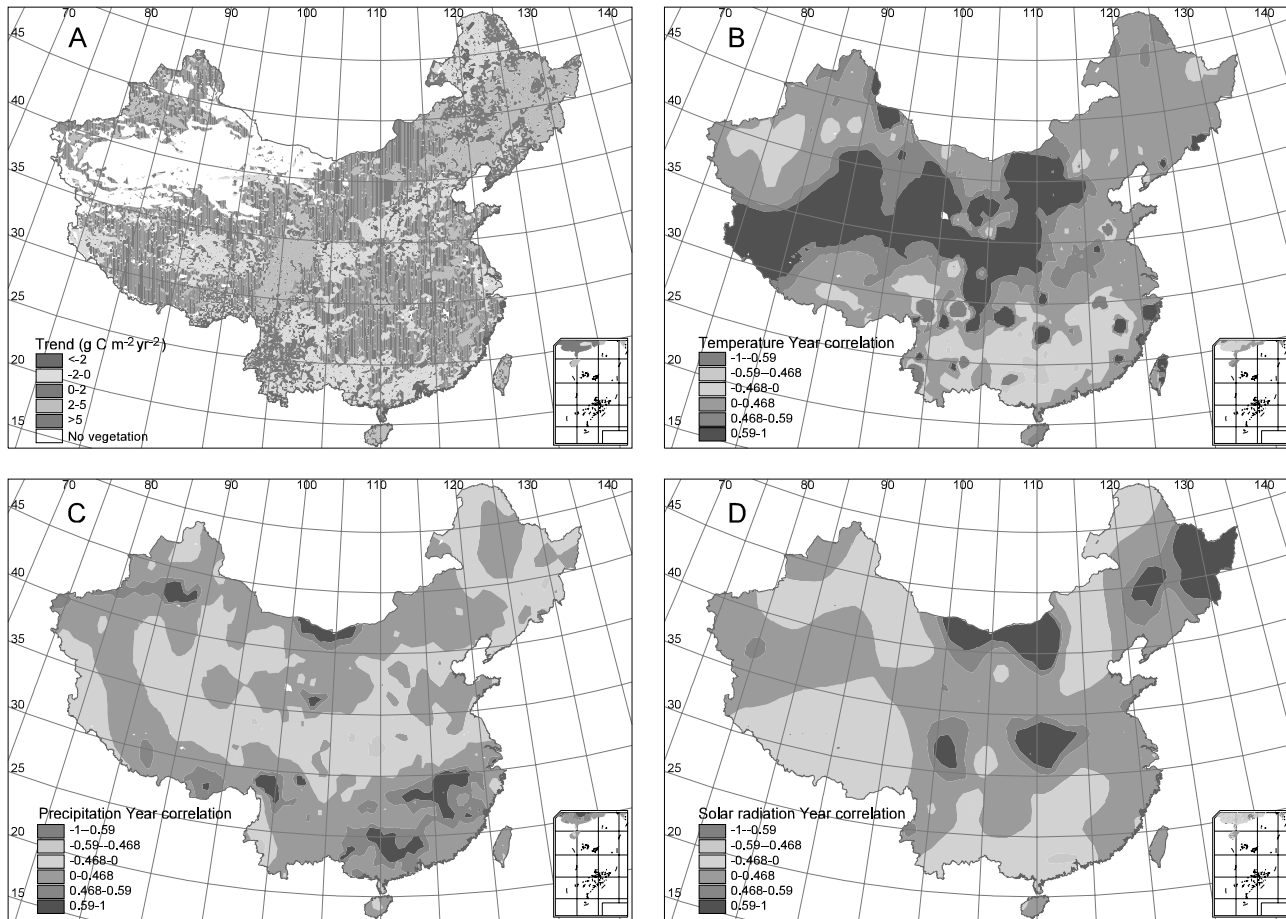


**Figure 6.** Spatial patterns of (a) trends in CASA-derived mean NPP, and coefficients of correlation (b) between temperature and time, (c) between precipitation and time, and (d) between solar radiation and time for each grid cell for summer in China. See color version of this figure at back of this issue.

an-ling Mountains in northeast China, eastern Tibet and southwestern Sichuan Province, Tianshan Mountains in northwest China, and part of middle and lower Yangtze River. The NPP increase in northwest China was coupled with the increased summer precipitation (Figure 6c), whereas in other areas it may be associated with the increased summer temperature (Figure 6b) and summer solar radiation (Figure 6d). Areas characterized by a decline in summer NPP included Da-xing-an-ling Mountains in northeast China, hilly areas of Guangdong and Guangxi Provinces, southeastern Yunnan-Guizhou Plateau, part of the Loess Plateau and the North China Plain, and part of the sources of the three rivers (i.e., the Yangtze River, the Yellow River, and the Lancang River), where the decline in NPP was parallel with that in temperature, precipitation, and solar radiation (Figures 6b, 6c, and 6d). The summer precipitation in the Loess Plateau, the North China Plain, and Da-xing-an-ling Mountains declined and the summer temperature in hilly areas of Guangdong and Guangxi Provinces, southeastern Yunnan-Guizhou Plateau decreased remarkably. Summer NPP in the Pearl River and Yangtze River deltas also declined, caused by rapid urbanization.

[28] In autumn, more than 95% of the whole study area exhibited a positive trend in mean temperature during the past 18 years (Figure 7b). The proportion of area with a significant increase in NPP and its magnitude is smaller than that in summer and spring (Figure 7a): the significant increase in NPP occurred in 11% of the study area, including the plain area of northeast China, northeastern part of Huanghuaihai Plain, eastern Tibet and western Sichuan Province, and Tianshan Mountains in northwest China. In contrast, in the upper reach of the three large rivers (i.e., Yangtze River, Yellow River, and Lancang River), southwestern Tibet, and part of the Sichuan Basin, autumn NPP exhibited an insignificant decline.

[29] Figure 8 illustrates spatial distribution of seasons with the largest increase in seasonal mean NPP during 1982 to 1999. About 53% of the total area with the largest NPP increase occurred in summer; they included northwest China, most parts of the Tibetan Plateau and northeast China, the Sichuan Basin, and part of the middle and lower reaches of Yangtze River. Thirty-two percent of the total area with the largest NPP increase appeared in spring (including Da-xing-an-ling Mountains, hilly areas of Guangdong and Guangxi Provinces, and

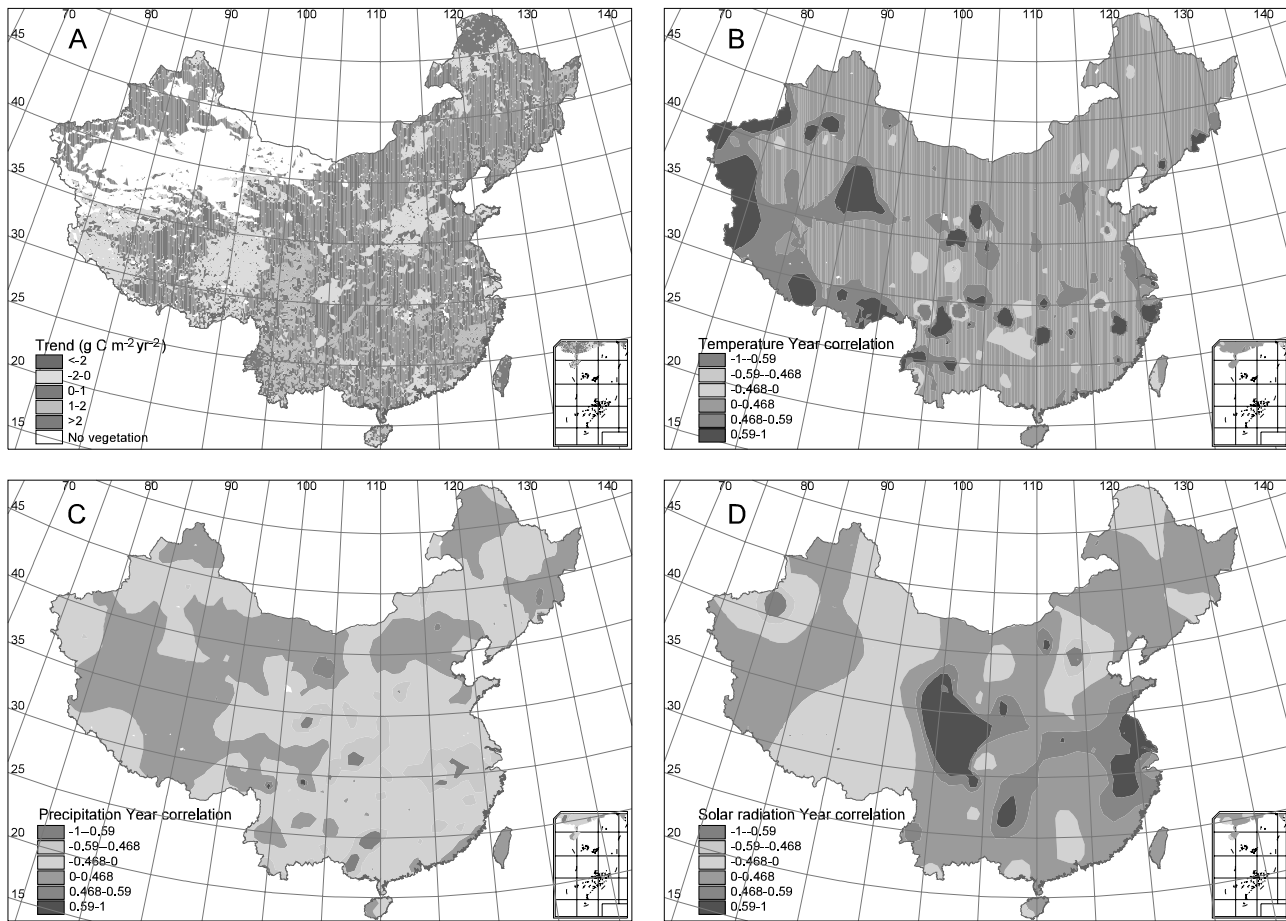


**Figure 7.** Spatial patterns of (a) trends in CASA-derived mean NPP, and coefficients of correlation (b) between temperature and time, (c) between precipitation and time, and (d) between solar radiation and time for each grid cell for autumn in China. See color version of this figure at back of this issue.

part of southeastern Yunan-Guizhou Plateau), whereas only 12% was in autumn. Parts of the Pearl River delta, the Yangtze River delta, and the Loess Plateau experienced a significant decline in NPP during the whole growing season.

### 3.3. Monthly NPP Trends

#### 3.3.1. Monthly Trends at the Country Scale

[30] We analyze monthly NPP trends and their contributions to annual NPP increase to explore possible mechanisms for the NPP trends. Figure 9a shows the seasonal changes in monthly NPP in the early 1980s (average of 1982–1984) and late 1990s (average of 1997–1999). The NPP of each month was larger in the late 1990s than that in the early 1980s, and such increase was more remarkable in the first half-year. The timing of peak NPP advanced from August in the early 1980s to July by the late 1990s, implying that the magnitude and rate of NPP increase in July were greater than those in August.

[31] Figure 9b shows the magnitude and rate of annual mean increase in monthly NPP over the 18 years. The monthly NPP trends were positive for all months, indicating that mean NPP has increased in every month over the study

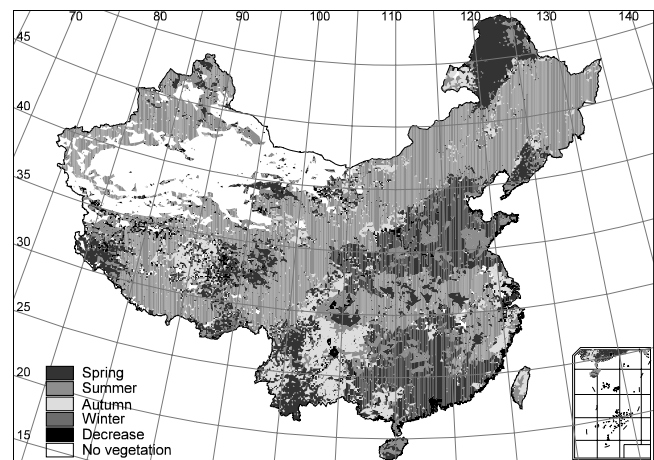


**Figure 8.** Spatial distribution of season with the largest increase in seasonal mean NPP derived from CASA during 1982–1999. See color version of this figure at back of this issue.

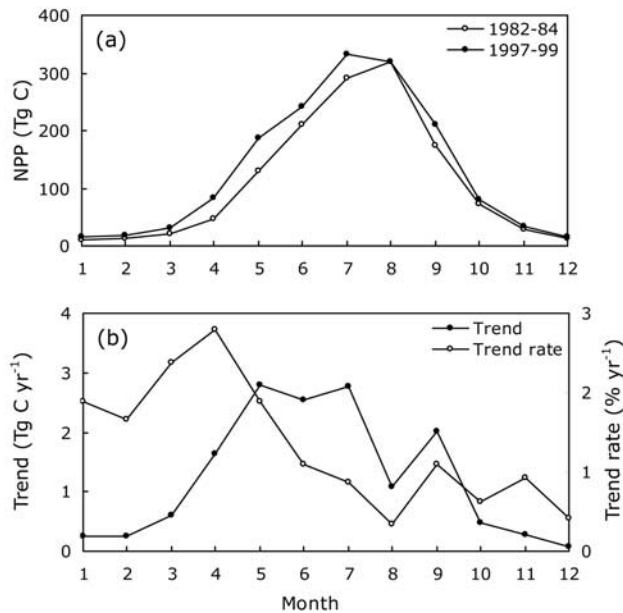


**Figure 9.** Changes in monthly mean NPP derived from CASA and its trends in China from 1982 to 1999. (a) Three-year averaged monthly mean NPP for 1982–1984 and 1997–1999. (b) Magnitude and rate of annual mean increase in monthly NPP over the 18 years.

period. A larger NPP rise (above 2.5 Tg C yr<sup>-1</sup>) occurred in May, June, and July, accounting for 18.9%, 17.2%, and 18.7% of the total annual NPP increase, respectively, while January, February, November, and December saw a much smaller trend less than 0.5 Tg C yr<sup>-1</sup>, only accounting for about 6% of the total annual NPP increase. The largest increase rate of monthly NPP in March, April, and May (above 1.5% yr<sup>-1</sup>) revealed the largest NPP increase rate in spring, while the increase rates for summer and autumn were relatively small, with less than 1% yr<sup>-1</sup> for most months.

### 3.3.2. Monthly Trends by Vegetation Type

[32] Figure 10 shows the seasonal changes in monthly NPP trend and its rate, monthly mean temperature trend, and monthly mean precipitation trend over the 18 years by vegetation type. For most months, the monthly NPP showed increasing trends for all vegetation types. In general, the trend rate for all vegetation types peaked in spring months (March to May) with an increase rate of 1–5% yr<sup>-1</sup>, suggesting the largest increase rate of vegetation NPP in the early growing season. This increase might be associated with the rise in temperature over this area. Spring temperature experienced significant increase, except for deciduous needleleaf forests in March.

[33] The largest increase in monthly NPP for evergreen broadleaf forests appeared in April with a trend of 0.62 g C m<sup>-2</sup> yr<sup>-2</sup>, while that for deciduous broadleaf forests, evergreen needleleaf forests, deciduous needleleaf forests, and savannas occurred in May with a trend of 0.4–1.0 g C m<sup>-2</sup> yr<sup>-2</sup>. Furthermore, the trends for evergreen broadleaf forests, evergreen needleleaf forests, and broad-

leaf shrubs were also notable in September, ranging from 0.4 to 0.6 g C m<sup>-2</sup> yr<sup>-2</sup>.

[34] The largest increase in monthly NPP for broadleaf and needleleaf mixed forests, temperate grasslands, alpine meadows and tundra, deserts, and cultivation all occurred in summer. The June and July NPP trends for broadleaf and needleleaf mixed forests were the most significant among all vegetation types, with 1.3 and 1.6 g C m<sup>-2</sup> yr<sup>-2</sup>, respectively. The increased NPP in summer for this forest type and alpine meadows was likely primarily a result of increased summer temperatures (Figures 10c and 10i); however, changes in NPP for deserts and temperate grasslands could be associated with variations in precipitation (Figures 10g and 10j). Most vegetated areas (except deciduous broadleaf forests, broadleaf and needleleaf mixed forests, and deciduous needleleaf forests) experienced a rise in summer precipitation, and, in particular, temperate grasslands and deserts suffered a significant increase in July precipitation.

## 4. Discussion

### 4.1. Total Annual NPP Trends

[35] Results from observed atmospheric CO<sub>2</sub> and O<sub>2</sub> concentrations [Ciais *et al.*, 1995; Keeling *et al.*, 1996; Bousquet *et al.*, 2000], inventory data [Fang *et al.*, 2001b; Pacala *et al.*, 2001], remote sensing data [Myneni *et al.*, 1997a; Tucker *et al.*, 2001; Zhou *et al.*, 2001; Piao *et al.*, 2003; Slayback *et al.*, 2003], and carbon process models [Dai and Fung, 1993; Malmström *et al.*, 1997; Tian *et al.*, 1998; Peng and Apps, 1999; Randerson *et al.*, 1999; Schimel *et al.*, 2000; Hicke *et al.*, 2002a; Lucht *et al.*, 2002; Cao *et al.*, 2003; Fang *et al.*, 2003] have all suggested that terrestrial vegetation NPP of the Northern Hemisphere has increased over the past 2 decades and, as a result, the northern terrestrial ecosystems have become important sinks for atmospheric CO<sub>2</sub>. However, these results differed greatly in the magnitude and spatial distribution of this NPP increase owing to differences in approaches and data sources [Keeling *et al.*, 1996; Myneni *et al.*, 1997a; Schimel *et al.*, 2000; Pacala *et al.*, 2001; Schimel *et al.*, 2001]. For example, with use of a satellite-based model, Nemani *et al.* [2003] reported that NPP increased by 6.17% (3.4 Pg C) over the past 18 years globally, while this value was 10% during the 1980s based on work by Malmström *et al.* [1997], Potter *et al.* [1999], and Ichii *et al.* [2001], which was larger than that expected from the fertilization effect of elevated CO<sub>2</sub> [Thompson *et al.*, 1996]. Our results suggested that terrestrial NPP in China increased at a rate of 0.015 Pg C yr<sup>-2</sup> over the period 1982–1999, corresponding to a total increase of 18.5%, or 1.03% annually, which is larger than that in North America (8% during 17 years) [Hicke *et al.*, 2002b].

[36] The well-documented food yield statistics support that the large NPP increase occurred in China's terrestrial ecosystems. The food-yield statistics [Editorial Committee for China's Agricultural Yearbook, 2000] indicate that the trend for total food yield (3.89 Tg C yr<sup>-2</sup>) is closely correlated to that of CASA-derived crop NPP (3.68 Tg C yr<sup>-2</sup>), although the magnitude of the former was smaller than that of the latter because food yield was only a portion of total NPP for food crops [Fang *et al.*, 2003]. Such a large

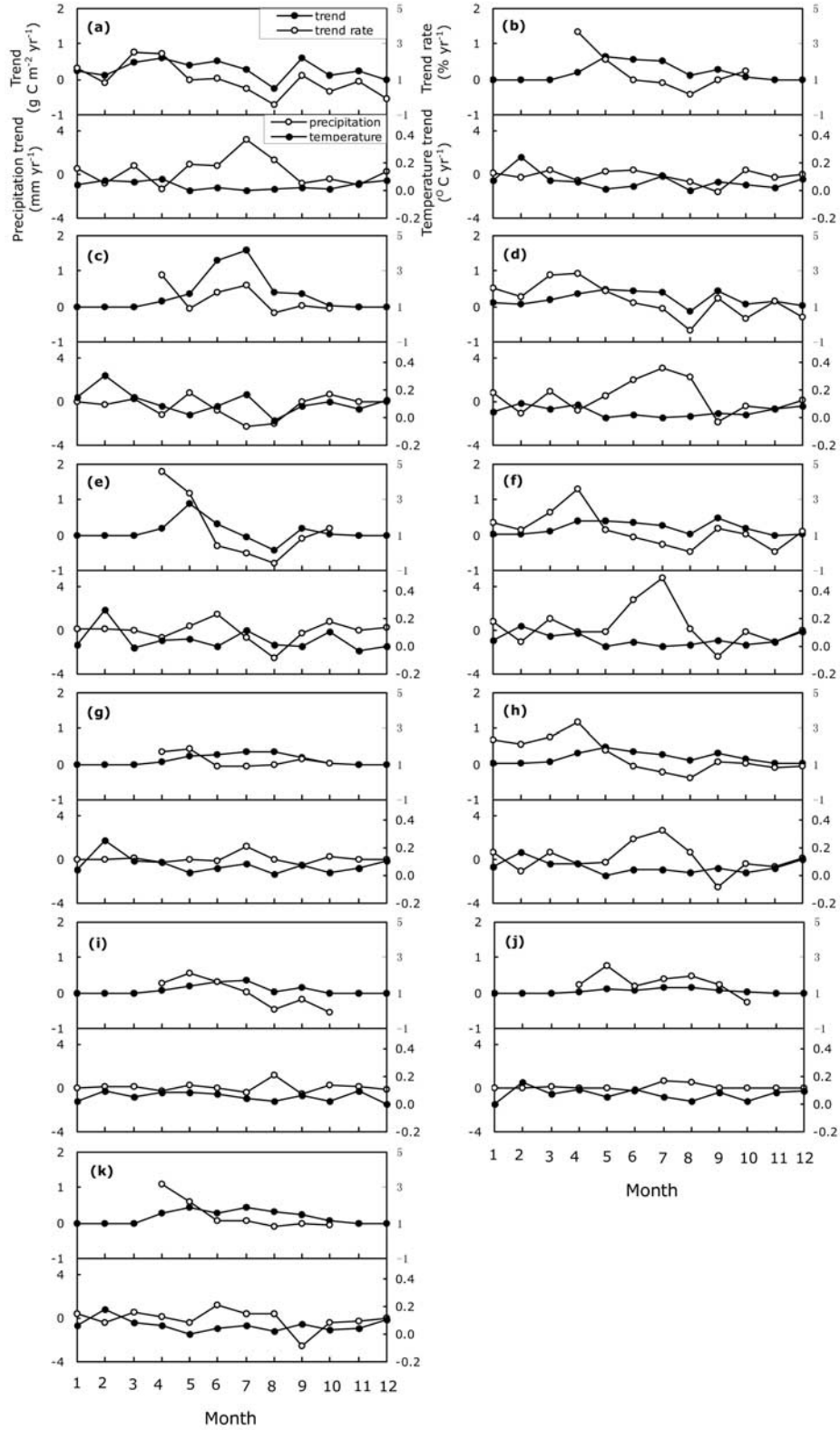


**Figure 10.** Seasonal changes in magnitude of monthly CASA-derived NPP trend and its rate, monthly mean temperature trend, and monthly mean precipitation trend over the 18 years by vegetation type in China. (a) Evergreen broadleaf forests. (b) Deciduous broadleaf forests. (c) Broadleaf and needleleaf mixed forests. (d) Evergreen needleleaf forests. (e) Deciduous needleleaf forests. (f) Broadleaf shrubs. (g) Temperate grasslands. (h) Savannas. (i) Alpine meadows and tundra. (j) Deserts. (k) Cultivation.

NPP increase calculated from CASA can also be evidenced from nationwide forest inventory surveys during the 1980–1998 [Fang *et al.*, 2001b].

[37] Climate change is probably a major controller for year-to-year variations in vegetation activity [Schimel *et al.*, 2001; Zhou *et al.*, 2001; Lucht *et al.*, 2002]. At the national level, the interannual variation in annual NPP was correlated with annual mean temperature ( $R^2 = 0.52$ ,  $p = 0.001$ ) but not with annual precipitation in our study area. However, the annual NPP was significantly correlated with summer precipitation ( $R^2 = 0.35$ ,  $p = 0.01$ ), indicating that the allocation of precipitation within a year played a key role in determining the year-to-year variations of NPP. Although annual mean precipitation in China had no significant trend, summer (June to August) precipitation significantly increased ( $R^2 = 0.27$ ,  $p = 0.027$ ) and autumn precipitation significantly decreased ( $R^2 = 0.33$ ,  $p = 0.012$ ). This concurrent increase in both summer temperature and precipitation may have enhanced plant growth during the growing season in China.

#### 4.2. Spatial Patterns in NPP Trends

[38] The NPP trends showed a high degree of geographical heterogeneity but corresponded well to regional climate and land use/land cover changes. Over the past 18 years, a significant increase in NPP ( $>6 \text{ g C m}^{-2} \text{ yr}^{-2}$ ) occurred principally in the regions dominated by two monsoon climate systems, the southeast and the southwest monsoon, which bring abundant rainfall during the growing season from the Pacific Ocean and the Indian Ocean, respectively. Therefore, increased temperature and solar radiation in these regions will enhance plant growth and increase the vegetation NPP [Fang *et al.*, 2003].

[39] Tianshan Mountains in northwest China has experienced a significant rise in NPP, with the largest NPP increase in the study area. This increase could probably be attributed to the transition of the regional climate from warm-dry to warm-humid [Shi *et al.*, 2003; Fang *et al.*, 2004]. Precipitation data indicated that annual precipitation, especially summer precipitation, has significantly increased over the 2 decades in this region [Qin, 2002] (Figure 6c).

[40] NPP also increased significantly in the agricultural areas of eastern China, including parts of the North China Plain, the Northeast China Plain, and the Yangtze River Basin. The NPP increase in agricultural areas could result from not only climate changes, but also agricultural activities such as increased irrigation and fertilization in the recent several decades [Fang *et al.*, 2004].

[41] NPP significantly declined in the Pearl River and Yangtze River deltas owing mainly to the rapid urbanization over the past 2 decades [Liu *et al.*, 2003]. Urban expansion has also caused loss of croplands [Li *et al.*, 2003], and therefore resulted in the largest portion of areas (1.4%) with significant decrease in NPP in the cultivated regions.

[42] Deciduous needleleaf forest in the Da-xing-an-ling Mountains was the only vegetation type with no significant increase in annual NPP. Over the 18 years, although temperature showed a substantial rise, NPP only increased significantly in 8.9% of the study area, possibly associated

with deforestation [Wang *et al.*, 2002] and heavy forest fire in 1987 [Zhou, 1997].

#### 4.3. Temporal Patterns in NPP Trends

[43] The CASA-derived NPP has been extensively validated against both seasonal patterns of atmospheric  $\text{CO}_2$  measurements at sampling stations around the world [Denning, 1994; Potter *et al.*, 1999], and against multiyear estimates of NPP from field stations and tree rings [e. g., Malmström *et al.*, 1997; Hicke *et al.*, 2002a, 2002b; Lobell *et al.*, 2002; Fang *et al.*, 2003]. Although the CASA has been widely used to investigate interannual variations in total annual NPP [e.g., Malmström *et al.*, 1997; Potter *et al.*, 1999; Hicke *et al.*, 2002a, 2002b; Fang *et al.*, 2003; Nemani *et al.*, 2003], it is also structurally designed to estimate seasonal patterns in vegetation NPP [Potter *et al.*, 1993; Field *et al.*, 1995], and thus is used to explore changes in vegetation production in different temporal scales. For example, Denning [1994] analyzed the relationship between seasonal patterns of CASA-NPP and atmospheric  $\text{CO}_2$  measurements and found a good coincidence between these two measures. Randerson *et al.* [1999] compared seasonal changes in  $\text{CO}_2$  concentration with those in CASA-derived NPP. Hicke *et al.* [2002a] used the model to estimate monthly and seasonal NPP trends in North America over 1982–1998, as well as interannual NPP trend.

[44] To further illustrate the implications of the CASA in investigating the seasonal changes in NPP in different temporal scales, we used unpublished long-term monthly aboveground biomass measurements observed in a temperate grassland to compare monthly dynamics of measured NPP with those of CASA-simulated NPP. The monthly aboveground biomass data set was measured in a typical temperate grassland site in Inner Mongolia, China, dominated by *Stipa grandis* and *Leymus chinense*, from 1983 to 1999 (Z. L. Liu, unpublished data, 1983–1999). The data set enables comparison between directly measured and CASA-simulated NPP because biomass is usually used as an indicator of NPP in the grassland ecosystems. Figure 11 shows changes in monthly aboveground biomass for May to September over 1983–1999, and simulated monthly NPP over 1982–1999. In Figure 11a, each point represented an average of 20 plots of  $1 \text{ m}^2$ ; and in Figure 11b the monthly CASA-NPP was simulated using historical ground observations (such as monthly temperature, precipitation, and solar radiation, and information on soil) at around the study site. A general consistency can be found between these two NPP trends for each month, suggesting a potential applicability of the CASA in exploring seasonal NPP dynamics, although more evidence for this is required.

[45] In the present study, we examined the temporal changes in the CASA-derived NPP at different temporal (annual, seasonal and monthly) scales, and found that NPP increased at all the temporal scales over the past decades at the national spatial level. The increase in annual NPP is possibly a result of enhanced amplitude of the seasonal NPP cycle and lengthened period of growing season. The former was probably due to the rise in atmospheric  $\text{CO}_2$  concentration, elevated temperature, and increased atmospheric N and P deposition, and the latter likely resulted from ad-

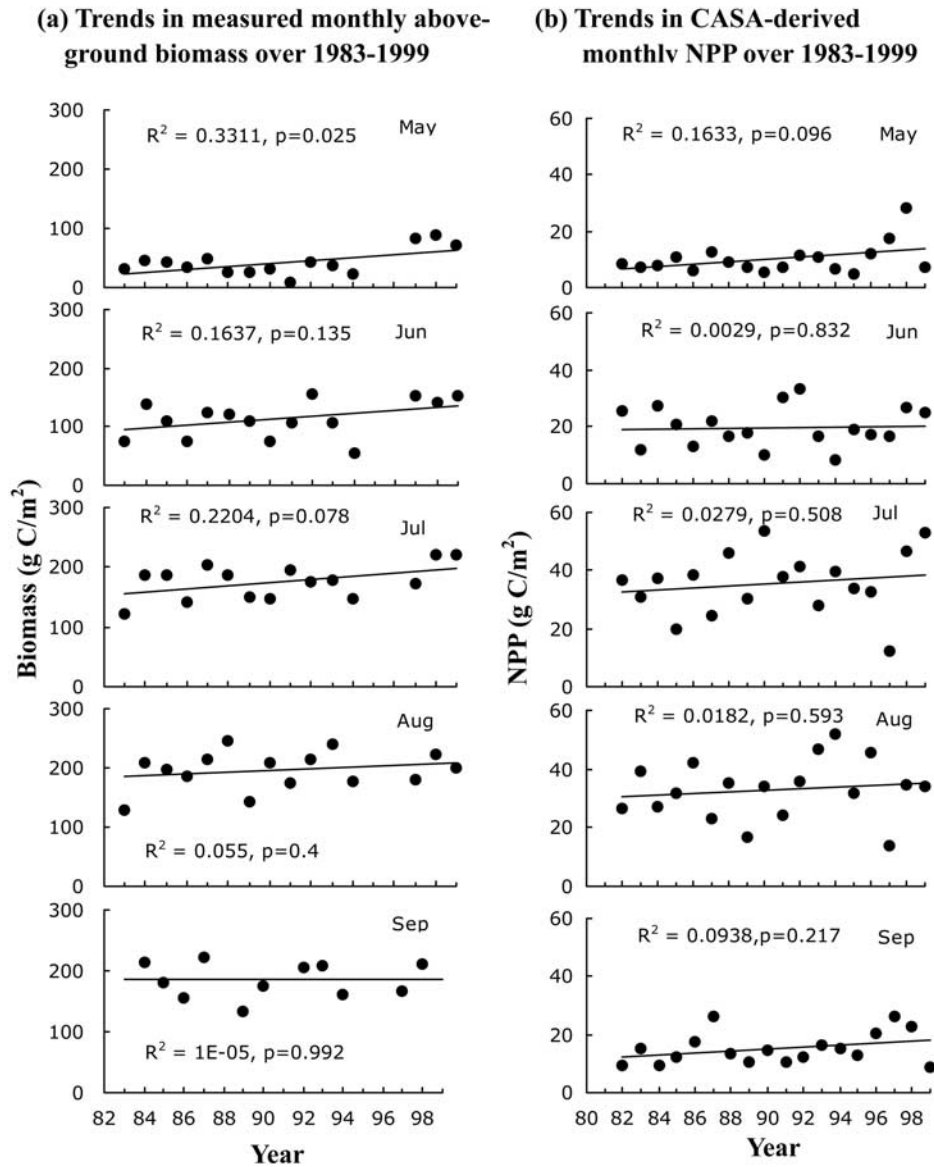


**Figure 11.** Changes in (a) monthly aboveground biomass for May to September in a typical temperate grassland site in Inner Mongolia over 1983–1999 (based on unpublished data, 1983–1999, from Z. L. Liu), and (b) CASA-simulated monthly NPP for May to September, calculated based on historical ground observations at around the biomass measurement site over 1982–1999.

vanced spring onset and extended autumn growth owing to climate warming [Keeling *et al.*, 1996; Randerson *et al.*, 1999; Hicke *et al.*, 2002a]. Seasonal changes in NPP in China indicated that NPP increase in summer (June to August), with an increase of  $6.4 \text{ Tg C yr}^{-2}$ , contributed most to that in the whole year (accounting for 43.2% of the total annual increase), while only 0.4% of NPP increase occurred in winter (December to February). 33.7% and 18.7% of total annual NPP increase came from early (March to May) and late growing seasons (September to November) (Table 1). This suggests that the increase in NPP stemmed primarily from enhanced vegetation activity during the

middle of the growing season (summer), and secondarily from the early growth season (spring) in China.

[46] At the national and biome scales, the increase rates of NPP in spring (above  $1.5\% \text{ yr}^{-1}$ ) were larger than those in other seasons, indicating that spring had the largest NPP increase rate among all the four seasons. The pronounced spring increase in NPP followed noticeable spring warming, which drives advanced growing seasons [Keeling *et al.*, 1996; Myneni *et al.*, 1997a; Tucker *et al.*, 2001; Zhou *et al.*, 2001].

[47] The changes in the phase of China's monthly NPP curve may be primarily the result of differences in the

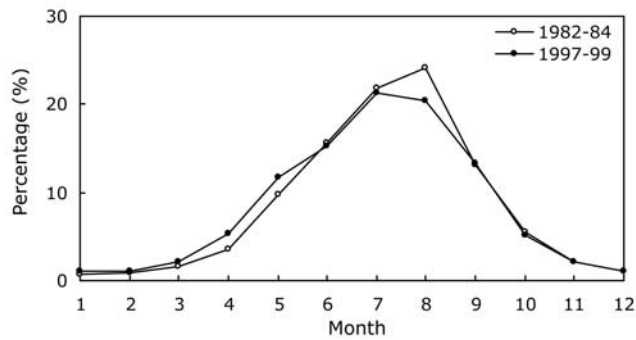


**Figure 12.** Seasonal changes in percentage of monthly NPP to annual NPP derived from CASA during 1982–1984 and 1997–1999.

magnitude and rate of increase in monthly NPP at different months. At the country scale, because of larger magnitude and rate of increase in NPP in July than in August (Figure 9b), the timing of peak NPP advanced from August in the early 1980s to July in the end of 1990s (Figure 9a). The annual mean increase in summer NPP was larger than that in winter NPP and, as a result, the amplitude of the seasonal NPP curve enhanced by 2.3% over the 18 years, which may indirectly explain the enhanced amplitude and advanced timing of the seasonal cycle of atmospheric CO<sub>2</sub> concentration [Keeling *et al.*, 1996]. In addition, the seasonal cycle of the percentage of monthly NPP to annual NPP depicted that the percentage of NPP in spring season (March to May) was obviously larger in the late 1990s (1997–1999) than that in the early 1980s (1982–1984), while that in July and August were smaller in the former than in the latter (Figure 12).

#### 4.4. Limitations and Next Steps

[48] The inherent limitation of ecosystem models derived from satellite data is the calibrated NDVI data set needed as input to the models [Asner *et al.*, 2000; Hicke *et al.*, 2002a]. If the NDVI product was clean of atmospheric and satellite signal degradation, these models would provide an excellent diagnostic of interannual NPP variation [Ciais *et al.*, 2001]. Although considerable efforts have been made for corrections, some variations due to satellite drift/changeover and incomplete corrections for calibration loss and atmospheric effects (clouds, aerosols, etc.) may still remain in the GIMMS NDVI data set.

[49] Another possible limitation of NDVI is that NDVI saturates in the case of dense leaf canopies. NDVI is usually used as a proxy of leaf area index (LAI) of vegetation canopy, and the change in LAI is nearly linear with NDVI until the LAI exceeds values of 3–4 m<sup>2</sup>/m<sup>2</sup>, above which NDVI rapidly approaches an asymptotic limit [Carlson and Ripley, 1997]. However, the CASA can reduce the effects of saturated closed canopy because it uses FPAR but not LAI to estimate NPP. Many studies have revealed that a stronger correlation exists between FPAR and NDVI than that between LAI and NDVI [e.g., Fensholt *et al.*, 2004], and that the NDVI-FAPAR rela-

tionship tends to be linear at a large spatial scale [Myneni *et al.*, 1997b]. Moreover, NDVI saturates primarily in the case of dense leaf canopies in humid tropical forests and old growth forests [Dong *et al.*, 2003; Asner *et al.*, 2004], while this area is very small in China (<3% of total country area) and occurs mainly in southeast Tibet and southern Yunnan, southernmost China [Editorial Committee for China's Vegetation, 2001]. Therefore, although in these regions NPP may be underestimated, such effect on the NPP change at the country level may be neglected.

[50] In addition, calculation of soil water balance in the CASA is one of the possible limitations because the model uses a one-layer bucket model [Potter *et al.*, 1993]. For this reason, our analysis focuses on direct NPP drivers (such as temperature, precipitation, solar radiation), but not on soil water balance.

[51] Finally, mechanisms other than climate, such as CO<sub>2</sub> fertilization, N deposition, and land-use change that affect NDVI, may also play roles in the increasing NPP trend [Schimel *et al.*, 2001]. However, these factors were not quantified in our study because they are not directly used in the CASA. How to separate the contributions to NPP increase attributed to different driving factors remains a great challenge for further studies.

## 5. Conclusions

[52] In the present study, we analyzed temporal and spatial variations in China's terrestrial NPP from 1982 to 1999 using CASA model, based on long-term satellite NDVI data set with high spatial resolution, climate and paired ground-based information on vegetation and soil. At the national level, annual NPP significantly increased from 1.33 Pg C yr<sup>-1</sup> in the early 1980s to 1.58 Pg C yr<sup>-1</sup> in the late 1990s with an annual mean increase magnitude of 0.015 Pg C. However, this change indicated a high degree of spatial heterogeneity, corresponding well to regional climate variations, and human activities. In general, increased temperature and solar radiation resulted in a large NPP increase in the southeast and southwest monsoon climates, while agricultural activities (such as irrigation and fertilization) have significantly contributed to an increase in NPP in agricultural areas. Rapid urbanization has caused a sharp decrease in NPP in the Pearl River and Yangtze River deltas, while deforestation and forest fire have likely made deciduous needleleaf forests in northeast China no significant increase in NPP.

[53] The total mean NPP for all four seasons indicated a significant increase at the national level. The areas with the largest NPP increase in summer accounted for 53.4% of the study area, while those in spring were 32% of the study area, indicating that the largest contribution to the annual NPP increase appeared in summer (43.2%), followed by spring (33.7%). The largest rate of NPP increase occurred in spring, presenting exact evidence for advanced growing season in China's terrestrial vegetation.

[54] The differences in the magnitude and rate of increase in monthly NPP have led to changes in the phase of China's seasonal NPP curve. At the country scale, the amplitude of the seasonal cycle of NPP has enhanced and the timing

of peak NPP has advanced, which is consistent with change in the seasonal cycle of observed atmospheric CO<sub>2</sub> concentration.

[55] Our findings of significantly increased terrestrial NPP in China over the past 2 decades are in relatively close agreement with field-based observations from forests and croplands, and thus provide country-scale evidence for increased growth of the northern terrestrial vegetation. On the other hand, annual and seasonal NPP trends show a large spatial and temporal heterogeneity, suggesting that the study of the spatial and seasonal responses of the vegetation NPP to climate changes is an important basis for further understanding the interactions between terrestrial ecosystems and the climatic systems and the mechanisms of increasing annual NPP.

[56] **Acknowledgments.** We thank Z. L. Liu at the University of Inner Mongolia (China) for providing an unpublished long-term monthly aboveground biomass data set, and C. Field, Y. Pan, and C. H. Peng for helpful comments and suggestions on this work. Thanks also are owed to W. H. Ma for preparing Figure 11. This research was supported by the National Natural Science Foundation of China (90211016 and 40021101), State Key Basic Research and Development Plan (G2000046801), and Peking University.

## References

- Asner, G. P., A. R. Townsend, and B. H. Braswell (2000), Satellite observation of El Niño effects on Amazon forest phenology and productivity, *Geophys. Res. Lett.*, *27*, 981–984.
- Asner, G. P., D. Nepstad, G. Cardinot, and D. Ray (2004), Drought stress and carbon uptake in an Amazon forest measured with spaceborne imaging spectroscopy, *Proc. Natl. Acad. Sci. U. S. A.*, *101*, 6039–6044.
- Behrenfeld, M. J., et al. (2001), Biospheric primary production during an ENSO transition, *Science*, *291*, 2594–2597.
- Bousquet, P., P. Peylin, P. Ciais, C. L. Quere, P. Friedlingstein, and P. P. Tans (2000), Regional changes in carbon dioxide fluxes of land and oceans since 1980, *Science*, *290*, 1342–1346.
- Cao, M.-K., S. D. Prince, K.-R. Li, B. Tao, J. Small, and X.-M. Shao (2003), Response of terrestrial carbon uptake to climate interannual variability in China, *Global Change Biol.*, *9*, 536–546.
- Carlson, T. N., and D. A. Ripley (1997), On the relation between NDVI, fractional vegetation cover, and leaf area index, *Remote Sens. Environ.*, *62*, 241–252.
- Chinese Climate Change National Research Group (2000), *Chinese Climate Change National Research*, Tsinghua Univ. Press, Beijing.
- Ciais, P., P. P. Tans, M. Troler, J. W. C. White, and R. J. Francey (1995), A large Northern Hemisphere terrestrial CO<sub>2</sub> sinks indicated by the <sup>13</sup>C/<sup>12</sup>C ratio of atmospheric CO<sub>2</sub>, *Science*, *269*, 1098–1102.
- Ciais, P., P. Friedlingstein, A. Friend, and D. S. Schimel (2001), Integrating global models of terrestrial primary productivity, in *Net Primary Production: Past, Present, and Future*, edited by J. Roy and H. Mooney, pp. 449–478, Elsevier, New York.
- Cramer, W., D. W. Kicklighter, A. Bondeau, B. Moore, C. Churkina, B. Nemry, A. Ruimy, and A. L. Schloss (1999), Comparing global models of terrestrial net primary productivity (NPP): Overview and key results, *Global Change Biol.*, *5*, Suppl. 1, 1–15.
- Cramer, W., et al. (2001), Global response of terrestrial ecosystem structure and function to CO<sub>2</sub> and climate change: Results from six dynamic global vegetation models, *Global Change Biol.*, *7*, 357–373.
- Dai, A., and I. Y. Fung (1993), Can climate variability contribute to the “missing” CO<sub>2</sub> sink?, *Global Biogeochem. Cycles*, *7*, 599–609.
- Denning, A. S. (1994), Investigations of the transport, sources, and sinks of atmospheric CO<sub>2</sub> using a general circulation model, Ph.D. dissertation, 336 pp., Dep. of Atmos. Sci., Colo. State Univ., Fort Collins.
- Dong, J., R. K. Kaufmann, R. B. Myneni, C. J. Tucker, P. E. Kauppi, J. Liski, W. Buermann, V. Alexeyev, and M. K. Hughes (2003), Remote sensing estimates of boreal and temperate forest woody biomass: Carbon pools, sources, and sinks, *Remote Sens. Environ.*, *84*, 393–410.
- Editorial Committee for China’s Agricultural Yearbook (ECCAY) (2000), *China’s Agricultural Yearbook 1982 to 1999*, China Agric. Press, Beijing.
- Editorial Committee for China’s Vegetation (2001), *Atlas of China’s Vegetation With a Scale of 1:100,000*, Science, Beijing.
- Fang, J. Y., S. L. Piao, Z. Y. Tang, C. H. Peng, and W. Ji (2001a), Relationship between interannual variability in net primary production and precipitation, *Science*, *293*, 1723.
- Fang, J. Y., A. P. Chen, C. H. Peng, S. Q. Zhao, and L. J. Ci (2001b), Changes in forest biomass carbon storage in China between 1949 and 1998, *Science*, *292*, 2320–2322.
- Fang, J. Y., Y. C. Song, H. Y. Liu, and S. L. Piao (2002), Vegetation-climate relationship and its application in the division of vegetation zone in China, *Acta Bot. Sin.*, *44*, 1105–1122.
- Fang, J. Y., S. L. Piao, C. B. Field, Y. D. Pan, Q. H. Guo, L. M. Zhou, C. H. Peng, and S. Tao (2003), Increasing net primary production in China from 1982 to 1999, *Front. Ecol. Environ.*, *1*, 293–297.
- Fang, J. Y., S. L. Piao, J. S. He, and W. H. Ma (2004), Increasing terrestrial vegetation activity in China, 1982–1999, *Sci. China, Ser. C*, *47*, 229–240.
- Fensholt, R., I. Sandholt, and M. S. Rasmussen (2004), Evaluation of MODIS LAI, fAPAR and the relation between fAPAR and NDVI in a semi-arid environment using in situ measurements, *Remote Sens. Environ.*, *91*, 490–507.
- Field, C. B., J. T. Randerson, and C. M. Malmström (1995), Global net primary production: Combining ecology and remote sensing, *Remote Sens. Environ.*, *51*, 74–88.
- Field, C. B., M. J. Behrenfeld, J. T. Randerson, and P. Falkowski (1998), Primary production of the biosphere: Integrating terrestrial and oceanic components, *Science*, *281*, 237–240.
- Gutman, G. (1999), On the use of long-term global data of land reflectances and vegetation indices derived from the Advanced Very High Resolution Radiometer, *J. Geophys. Res.*, *104*, 6241–6255.
- Haxeltine, A., and I. C. Prentice (1996), BIOME3: An equilibrium biosphere model based on ecophysiological constraints, resource availability and competition among plant functional types, *Global Biogeochem. Cycles*, *10*, 693–709.
- Hicke, J. A., G. P. Asner, J. T. Randerson, C. J. Tucker, B. Los, R. Birdsey, J. C. Jenkins, and C. B. Field (2002a), Trends in North American net primary productivity derived from satellite observations, 1982–1998, *Global Biogeochem. Cycles*, *16*(2), 1018, doi:10.1029/2001GB001550.
- Hicke, J. A., G. P. Asner, J. T. Randerson, C. J. Tucker, B. Los, R. Birdsey, J. C. Jenkins, C. B. Field, and E. Holland (2002b), Satellite-derived increases in net primary productivity across North America, 1982–1998, *Geophys. Res. Lett.*, *29*(10), 1427, doi:10.1029/2001GL013578.
- Holben, B. N. (1986), Characteristics of maximum value composite images from temporal AVHRR data, *Int. J. Remote Sens.*, *7*, 1417–1434.
- Ichii, K., Y. Matsui, Y. Yamaguchi, and K. Ogawa (2001), Comparison of global net primary production trends obtained from satellite-based normalized difference vegetation index and carbon cycle model, *Global Biogeochem. Cycles*, *15*, 351–363.
- Institute of Geography (1996), *Digitized Vegetation Map of China*, Natl. Lab. for GIS and Remote Sens., Beijing.
- Institute of Soil Science (1986), *The Soil Atlas of China*, Cartographic Publ. House, Beijing.
- Keeling, C. D., J. F. S. Chin, and T. P. Whorf (1996), Increased activity of northern vegetation inferred from atmospheric CO<sub>2</sub> measurements, *Nature*, *382*, 146–149.
- Li, X.-W., J.-Y. Fang, and S.-L. Piao (2003), Land use changes and its implication to the ecological consequences in lower Yangtze region, *Acta Geogr. Sin.*, *58*, 659–667.
- Liu, J., J.-M. Chen, J. Cihlar, and W. Chen (2002), Net primary productivity mapped for Canada at 1-km resolution, *Global Ecol. Biogeogr.*, *11*, 115–129.
- Liu, J.-Y., M.-L. Liu, D.-F. Zhuang, Z.-X. Zhang, and X.-Z. Deng (2003), Study on spatial pattern of land-use change in China during 1995–2000, *Sci. China, Ser. D*, *46*(4), 373–384.
- Lobell, D. B., J. A. Hicke, G. P. Asner, C. B. Field, C. J. Tucker, and S. O. Los (2002), Satellite estimates of productivity and light use efficiency in United States agriculture, 1982–98, *Global Change Biol.*, *8*, 722–735.
- Los, S. O. (1988), Estimation of the ratio of sensor degradation between NOAA AVHRR channel 1 and 2 from monthly NDVI composites, *IEEE Trans. Geosci. Remote Sens.*, *36*, 202–213.
- Lucht, W., I. C. Prentice, R. B. Myneni, S. Sitch, P. Friedlingstein, W. Cramer, P. Bousquet, W. Buermann, and B. Smith (2002), Climatic control of the high-latitude vegetation greening trend and Pinatubo effect, *Science*, *296*, 1687–1689.
- Malmström, C. M., M. V. Thompson, G. P. Juday, S. O. Los, J. T. Randerson, and C. B. Field (1997), Interannual variation in global-scale net primary production: Testing model estimates, *Global Biogeochem. Cycles*, *11*, 367–392.

- Melillo, J. M., A. D. McGuire, D. W. Kicklighter, B. Moore, C. J. Vorosmarty, and A. L. Schloss (1993), Global climate change and terrestrial net primary production, *Nature*, *363*, 234–240.
- Minnis, P., E. F. Harrison, L. L. Stowe, G. G. Gibson, F. M. Denn, D. R. Doelling, and W. L. Smith (1993), Radiative climate forcing by the Mount Pinatubo eruption, *Science*, *259*, 1411–1415.
- Monteith, J. L. (1977), Climate and efficiency of crop production in Britain, *Trans. R. Soc. London, Ser. B*, *281*, 271–294.
- Myneni, R. B., C. D. Keeling, C. J. Tucker, G. Asrar, and R. R. Nemani (1997a), Increased plant growth in the northern high latitudes from 1981–1991, *Nature*, *386*, 698–702.
- Myneni, R. B., R. R. Nemani, and S. W. Running (1997b), Estimation of global leaf area index and absorbed par using radiative transfer models, *IEEE Trans. Geosci. Remote Sens.*, *35*, 1380–1393.
- Myneni, R. B., J. Dong, C. J. Tucker, R. K. Kaufmann, P. E. Kauppi, J. Liski, L. M. Zhou, V. Alexeyev, and M. K. Hughes (2001), A large carbon sink in the woody biomass of northern forests, *Proc. Natl. Acad. Sci. U. S. A.*, *98*, 14,784–14,789.
- Nemani, R. R., C. D. Keeling, H. Hashimoto, W. M. Jolly, S. C. Piper, C. J. Tucker, R. B. Myneni, and S. W. Running (2003), Climate-driven increases in global terrestrial net primary production from 1982 to 1999, *Science*, *300*, 1560–1563.
- Ni, J. (2000), Net primary production, carbon storage and climate change in Chinese biomes, *Nord. J. Bot.*, *20*, 415–426.
- Pacala, S. W., et al. (2001), Consistent land- and atmosphere-based US carbon sink estimates, *Science*, *292*, 2316–2320.
- Parton, W. J., et al. (1993), Observations and modeling of biomass and soil organic matter dynamics for the grassland biome worldwide, *Global Biogeochem. Cycles*, *7*, 785–809.
- Peng, C.-H., and M. J. Apps (1999), Modelling the response of net primary productivity (NPP) of boreal forest ecosystems to changes in climate and fire disturbance regimes, *Ecol. Model.*, *122*, 225–238.
- Piao, S.-L., J.-Y. Fang, L.-M. Zhou, Q.-H. Guo, M. Henderson, W. Ji, Y. Li, and S. Tao (2003), Interannual variations of monthly and seasonal NDVI in China from 1982 to 1999, *J. Geophys. Res.*, *108*(D14), 4401, doi:10.1029/2002JD002848.
- Potter, C. S., J. T. Randerson, C. B. Field, P. A. Matson, P. M. Vitousek, H. A. Mooney, and S. A. Klooster (1993), Terrestrial ecosystem production: A process model based on global satellite and surface data, *Global Biogeochem. Cycles*, *7*, 811–841.
- Potter, C. S., S. Klooster, and V. Brooks (1999), Interannual variability in terrestrial net primary production: Exploration of trends and controls on regional to global scales, *Ecosystems*, *2*, 36–48.
- Potter, C., S. Klooster, M. Steinbach, P. Tan, V. Kumar, S. Shekhar, R. Nemani, and R. Myneni (2003), Global teleconnections of climate to terrestrial carbon flux, *J. Geophys. Res.*, *108*(D17), 4556, doi:10.1029/2002JD002979.
- Prince, S. D., and S. N. Goward (1995), Global net primary production: A remote sensing approach, *J. Biogeogr.*, *22*, 815–835.
- Qin, D.-H. (Ed.) (2002), *Assessment on Environment of Western China (Synopsis)*, Science Press, Beijing.
- Raich, J. W., E. B. Rastetter, and J. M. Melillo (1991), Potential net primary productivity in south America: Application of a global model, *Ecol. Appl.*, *1*, 399–429.
- Randerson, J. T., C. B. Field, I. Y. Fung, and P. P. Tans (1999), Increases in early season ecosystem uptake explain recent changes in the seasonal cycle of atmospheric CO<sub>2</sub> at high northern latitudes, *Geophys. Res. Lett.*, *26*(17), 2765–2768.
- Ruimy, A., B. Saugier, and G. Dedieu (1994), Methodology for the estimation of terrestrial net primary production from remotely sensed data, *J. Geophys. Res.*, *99*, 5263–5283.
- Running, S. W., and E. R. Hunt (1993), Generalization of a forest ecosystem process model for other biomes Biome-BGC, and an application for global-scale modes: Scaling processes between leaf and landscape levels, in *Scaling Physiological Processes: Leaf to Globe*, edited by J. R. Ehleringer and C. B. Field, pp. 141–158, Elsevier, New York.
- Schimel, D. S., et al. (2000), Contribution of increasing CO<sub>2</sub> and climate to carbon storage by ecosystems in the United States, *Science*, *287*, 2004–2006.
- Schimel, D. S., et al. (2001), Recent patterns and mechanisms of carbon exchange by terrestrial ecosystems, *Nature*, *414*, 169–172.
- Schulze, E. D., C. Wirth, and M. C. Heimann (2000), Climate change—Managing forests after Kyoto, *Science*, *289*, 2058–2059.
- Shi, Y.-F., Y.-P. Shen, D.-L. Li, G.-W. Zhang, Y.-J. Ding, R.-J. Hu, and E.-S. Kang (2003), Discussion on the present climate change from warm-dry to warm-wet in northwest China, *Quat. Sci.*, *23*(2), 152–164.
- Slayback, D., J. Pinzon, S. Los, and C. J. Tucker (2003), Northern Hemisphere photosynthetic trends 1982–1999, *Global Change Biol.*, *9*, 1–15.
- Stow, D. A., et al. (2004), Remote sensing of vegetation and land-cover change in Arctic tundra ecosystems, *Remote Sens. Environ.*, *89*, 281–308.
- Stowe, L. L., R. M. Garey, and P. P. Pellegrino (1992), Monitoring the Mt. Pinatubo aerosol layer with NOAA/11AVHRR data, *Geophys. Res. Lett.*, *19*, 159–162.
- Thompson, M. V., J. T. Randerson, C. M. Malmström, and C. B. Field (1996), Change in net primary production and heterotrophic respiration: How much is necessary to sustain the terrestrial carbon sink?, *Global Biogeochem. Cycles*, *10*, 711–726.
- Tian, H.-Q., J. M. Melillo, D. W. Kicklighter, A. D. McGuire, J. V. K. Helfrich, B. Moore, and C. J. Vorosmarty (1998), Effect of interannual climate variability on carbon storage in Amazonian ecosystems, *Nature*, *396*, 664–667.
- Tucker, C. J., W. W. Newcomb, and A. E. Dregne (1994), AVHRR data sets for determination of desert spatial extent, *Int. J. Remote Sens.*, *15*, 3547–3566.
- Tucker, C. J., D. Slayback, J. E. Pinzon, S. O. Los, R. B. Myneni, and M. G. Taylor (2001), Higher northern latitude NDVI and growing season trends from 1982 to 1999, *Int. J. Biometeorol.*, *45*, 184–190.
- Wang, S.-Q., H.-Q. Tian, J.-Y. Liu, D.-F. Zhuang, S.-W. Zhang, and W.-Y. Hu (2002), Characterization of changes in land cover and carbon storage in northeastern China: An analysis based on Landsat TM data, *Sci. China, Ser. C*, *45*, S40–S47.
- Zhai, P.-M., A.-J. Sun, F.-M. Ren, X.-N. Liu, B. Gao, and Q. Zhang (1999), Chances of climate extremes in China, *Clim. Change*, *42*, 203–218.
- Zhou, L.-M., C. J. Tucker, R. K. Kaufmann, D. Slayback, N. V. Shabanov, and R. B. Myneni (2001), Variations in northern vegetation activity inferred from satellite data of vegetation index during 1981 to 1999, *J. Geophys. Res.*, *106*(D17), 20,069–20,083.
- Zhou, L.-M., R. E. Dickinson, Y. Tian, M. Jin, K. Ogawa, H. Yu, and T. Schmugge (2003), A sensitivity study of climate and energy balance simulations with use of satellite-derived emissivity data over Northern Africa and the Arabian Peninsula, *J. Geophys. Res.*, *108*(D24), 4795, doi:10.1029/2003JD004083.
- Zhou, Y.-L. (1997), *Geography of the Vegetation in Northeast China*, Science Press, Beijing.

J. Fang (corresponding author), S. Piao, K. Tan, and B. Zhu, College of Environmental Sciences, Center for Ecological Research and Education, Peking University, Beijing 100871, China. (jyfang@urban.pku.edu.cn)

S. Tao, Key Laboratory for Earth Surface Processes of the Ministry of Education, Peking University, Beijing 100871, China.

L. Zhou, School of Earth and Atmospheric Sciences, Georgia Institute of Technology, Atlanta, GA 30332-0340, USA.

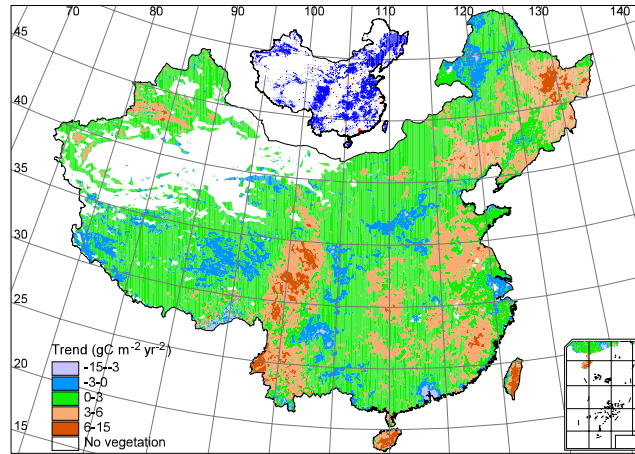


**Figure 2.** Spatial distribution of annual NPP trend calculated from CASA over 1982 to 1999. The insert map at top shows significant increase (blue) or decrease (red) in NDVI over the 18 years.

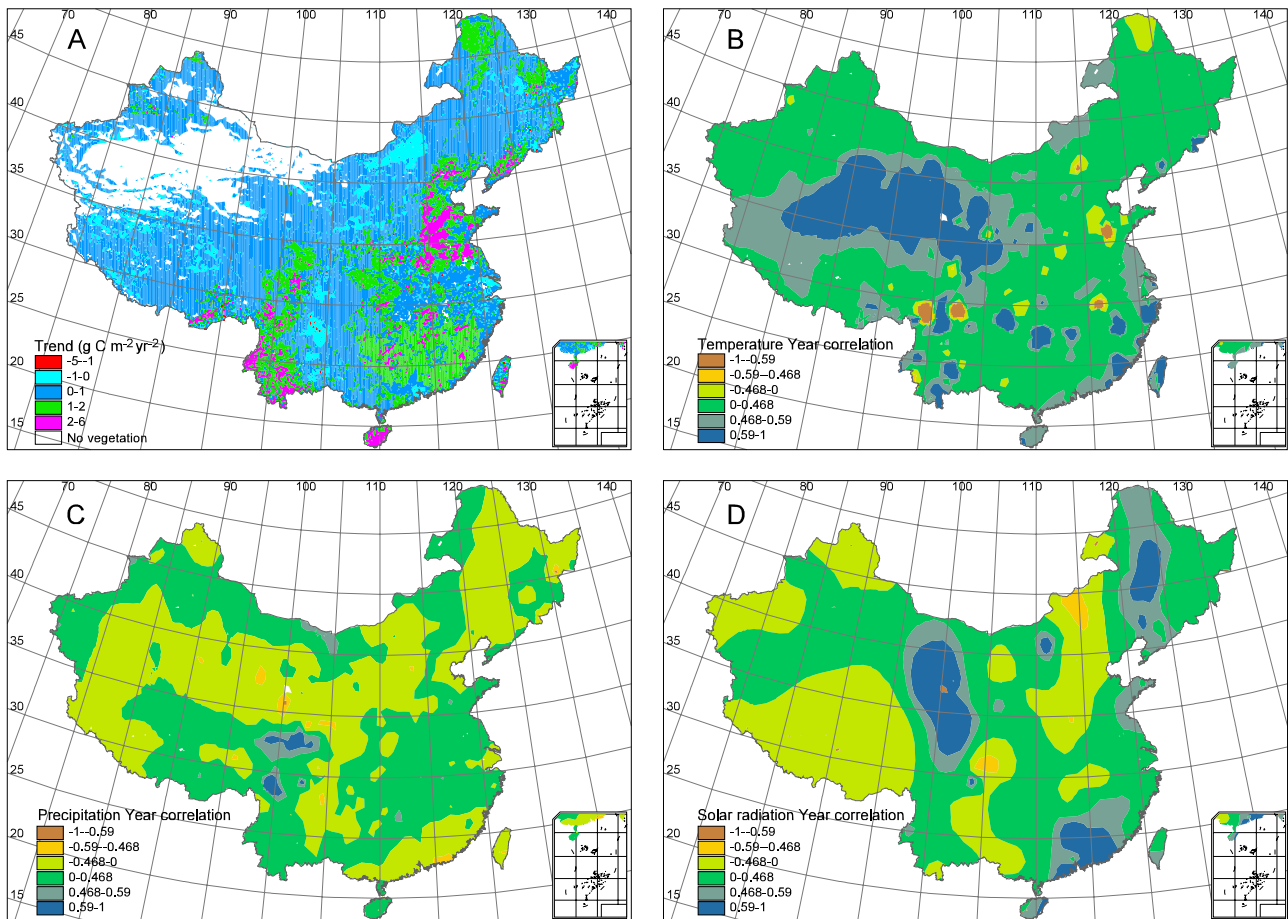


**Figure 5.** Spatial patterns of (a) trends in CASA-derived mean NPP, and coefficients of correlation (b) between temperature and time, (c) between precipitation and time, and (d) between solar radiation and time for each grid cell for spring (March to May) in China. The value of 0.468 and 0.59 for coefficient of correlation in the legend of Figures 5b, 5c, and 5d corresponds statistically to 5% and 1% significance levels, respectively.

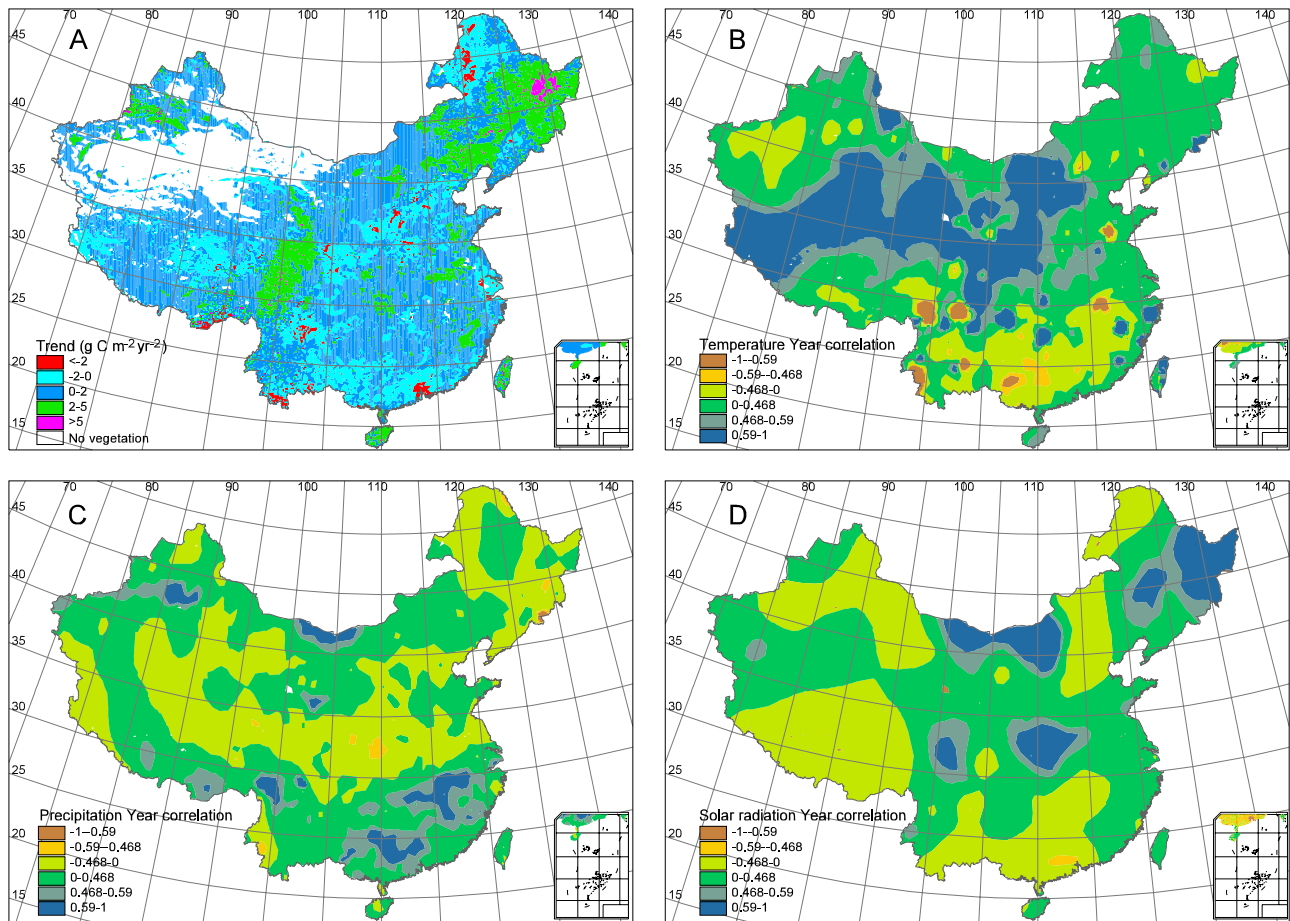


**Figure 6.** Spatial patterns of (a) trends in CASA-derived mean NPP, and coefficients of correlation (b) between temperature and time, (c) between precipitation and time, and (d) between solar radiation and time for each grid cell for summer in China.

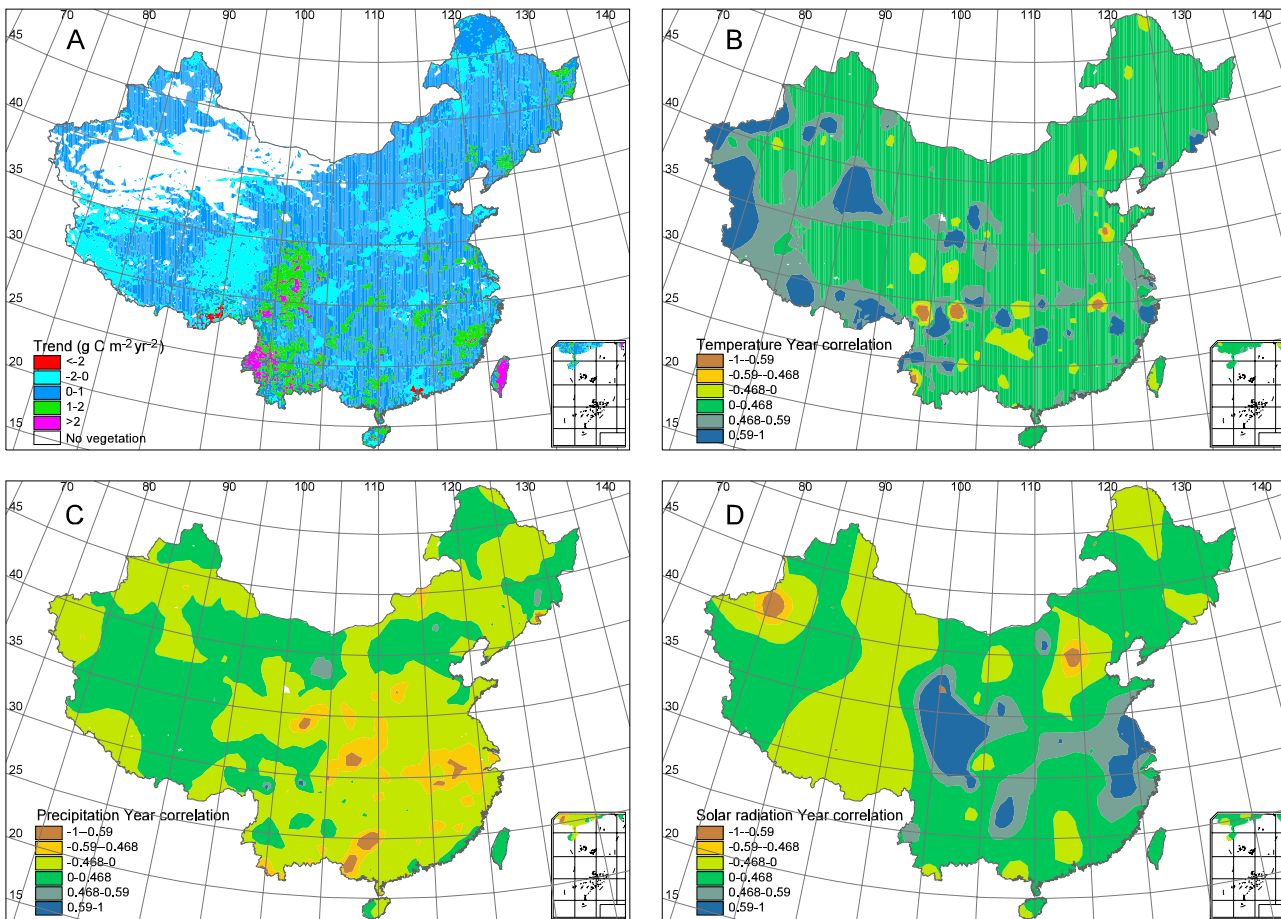


**Figure 7.** Spatial patterns of (a) trends in CASA-derived mean NPP, and coefficients of correlation (b) between temperature and time, (c) between precipitation and time, and (d) between solar radiation and time for each grid cell for autumn in China.

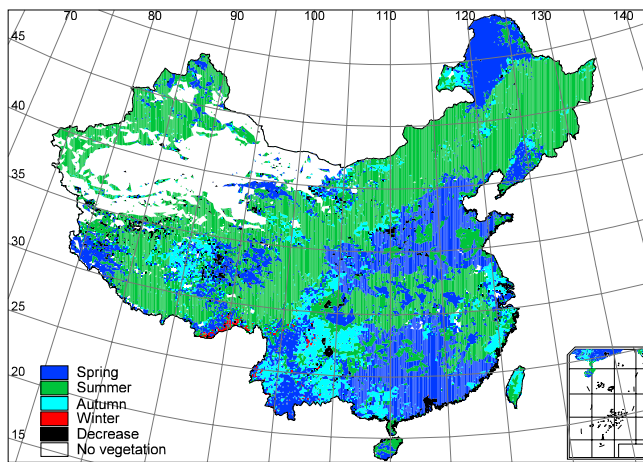


**Figure 8.** Spatial distribution of season with the largest increase in seasonal mean NPP derived from CASA during 1982–1999.